Function of histone methyltransferase EZH2 and development of EZH2 inhibitors

2022/12/01 Literature Seminar

M1 Mayu Onoda

Contents

Contents

▫ Structure of nucleosome

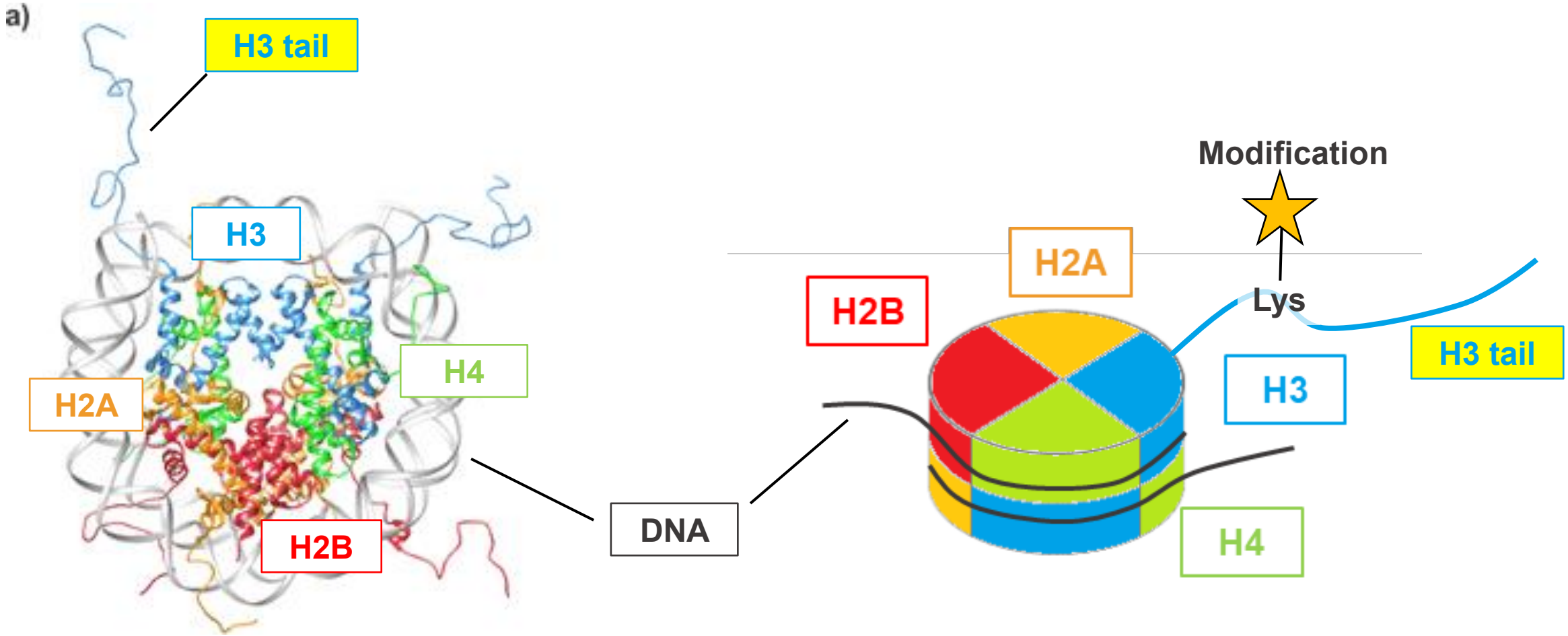

Müller, M. M.; Muir, T. W., *Chem. Rev.* **2015**, *115*, 2296.

▫ Modification (H3K27Me)

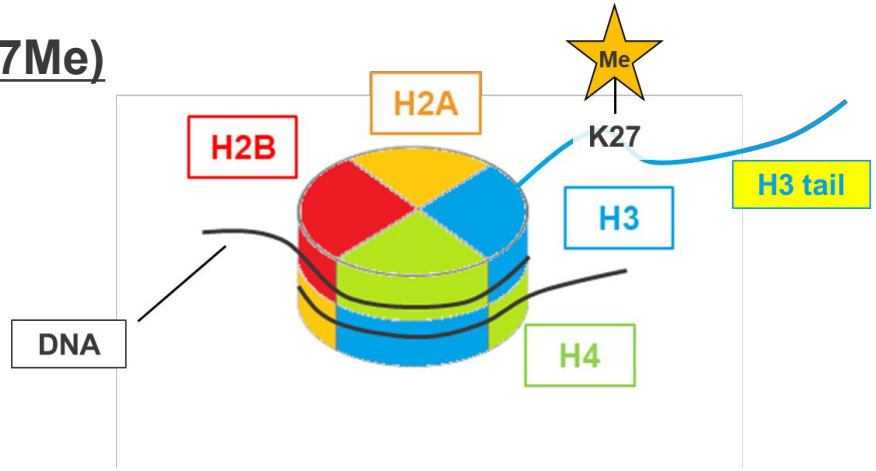

▫ Lysine residue methylation mechanism

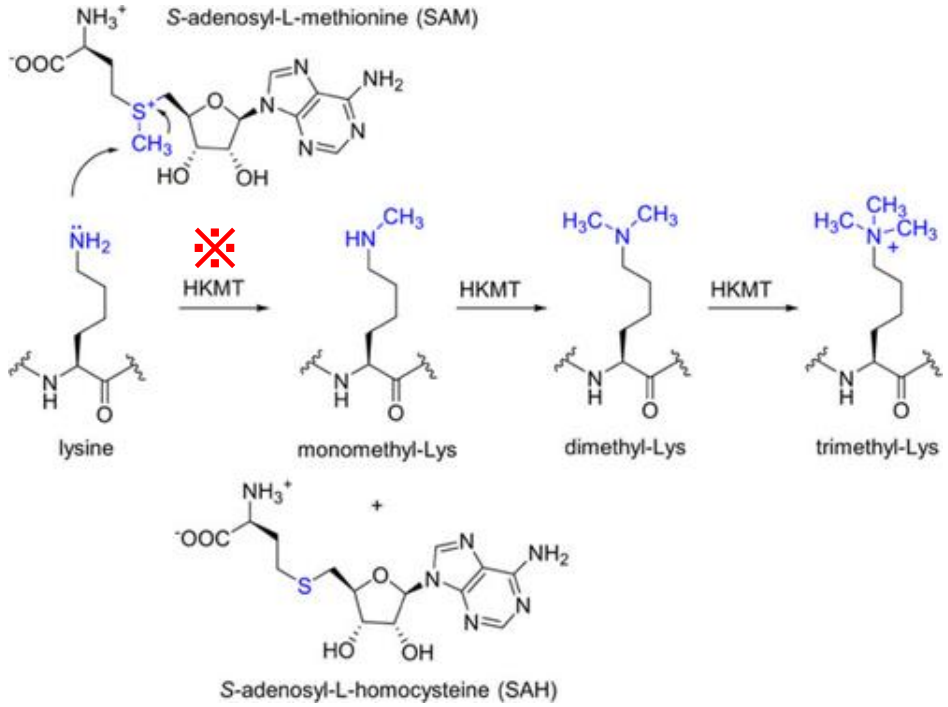

※ **HKMT**
= Histone Lysine Methyltransferase

R. Fioravanti et al, *Chem. Rec.* **2018**, *18*, 1818.

▫ **EZH2 forms a PRC2 complex.**

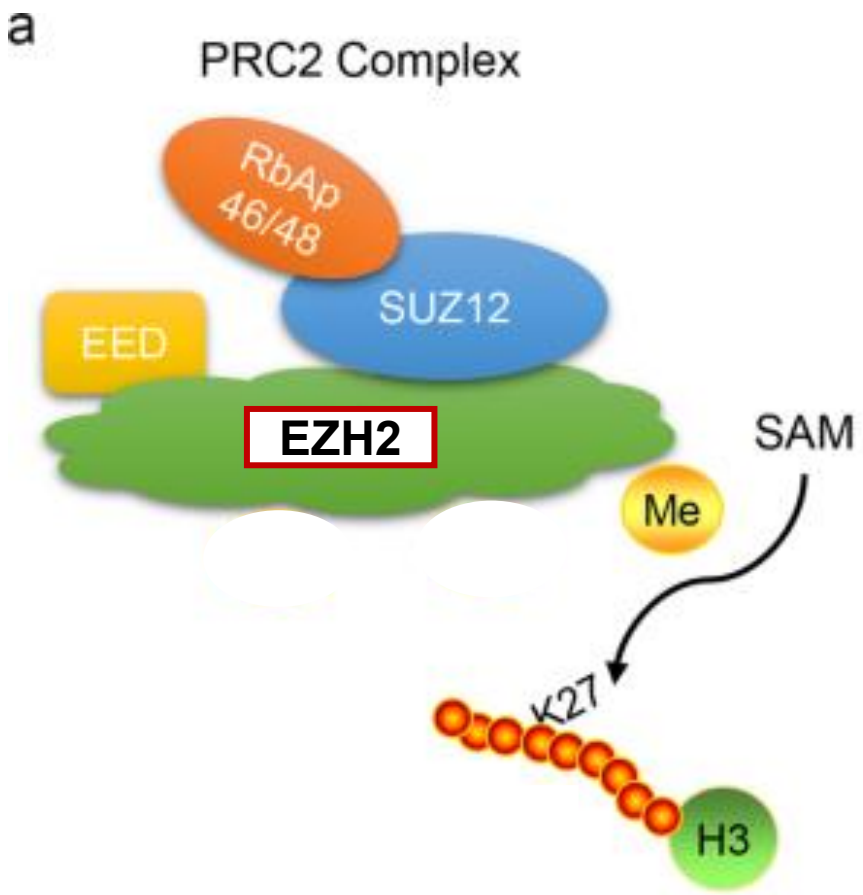

H3K27 Methylation

▫ **The SET domain of EZH2 catalyzes methylation.**

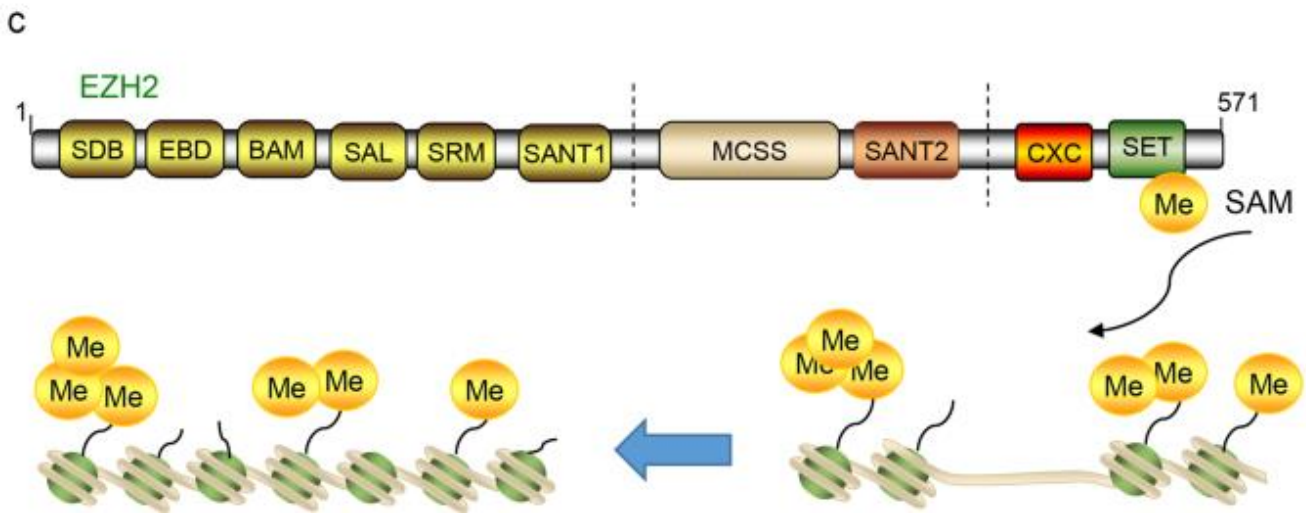

An, R., Li, YQ., Lin, YL. *et al, Cancer Gene Ther*, **2022**

EZH2 (H3K27 methyltransferase)

- **EZH2 (WT) and EZH2 (Mutant) prefer different methylation reactions.**

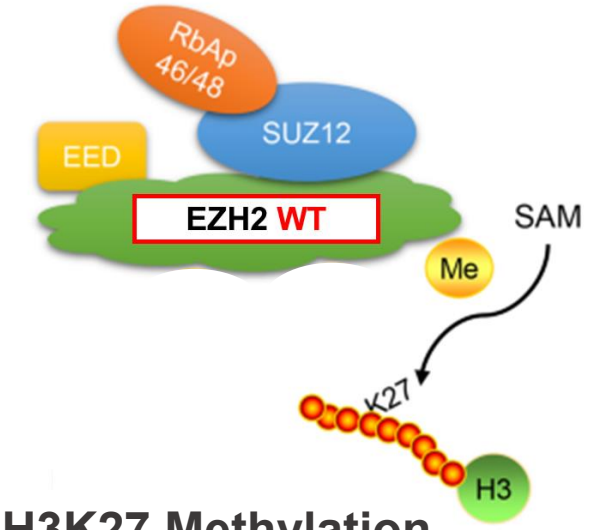

H3K27 Methylation

EZH2 (WT)
◎Me0→Me1
○Me1→Me2
△Me2→Me3

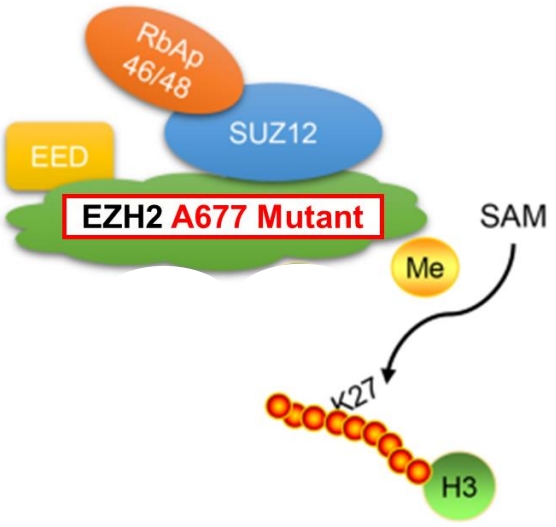

EZH2 (A677 Mut)
○Me0→Me1
○Me1→Me2
○Me2→Me3

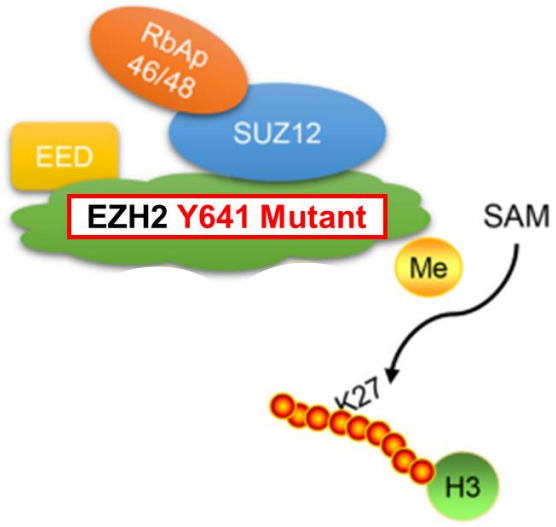

EZH2 (Y641 Mut)
△Me0→Me1
△Me1→Me2
◎Me2→Me3

What makes this difference?

McCabe M.T.et al, *Proc. Natl. Acad. Sci. USA,* **2012**, *109*, 2989.
An, R., Li, YQ., Lin, YL. *et al, Cancer Gene Ther*, **2022**

EZH2 (H3K27 methyltransferase)

EZH2 (WT)
◎Me0→Me1
○Me1→Me2
△Me2→Me3

EZH2 (A677 Mut)
○Me0→Me1
○Me1→Me2
○Me2→Me3

EZH2 (Y641 Mut)
△Me0→Me1
△Me1→Me2
◎Me2→Me3

What makes this difference?

Me0→Me1: Hydrogen bond is important.
Me2→Me3: Wide space is important.

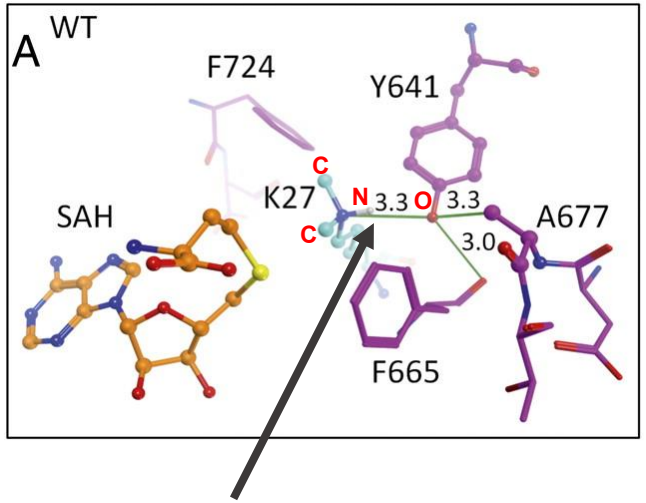

・Hydrogen bond
Tyr (O atom) & K27 (N atom)

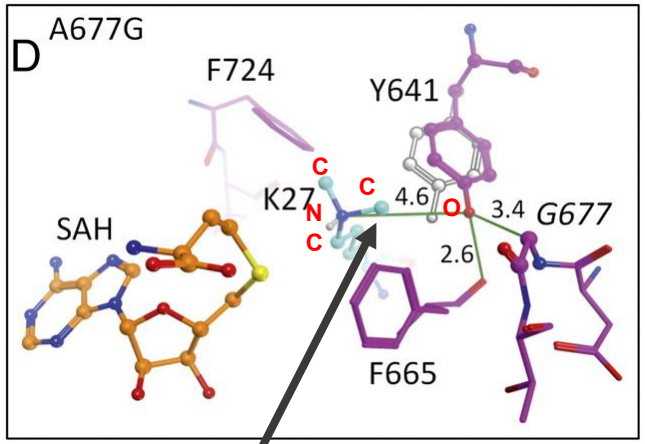

・Space is created.
・Hydrogen bond
Tyr (O atom) & K27 (N atom)

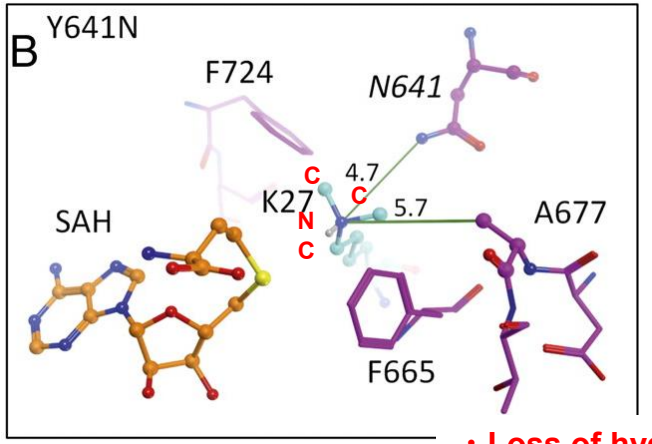

・Loss of hydrogen bond.
・Space is created.

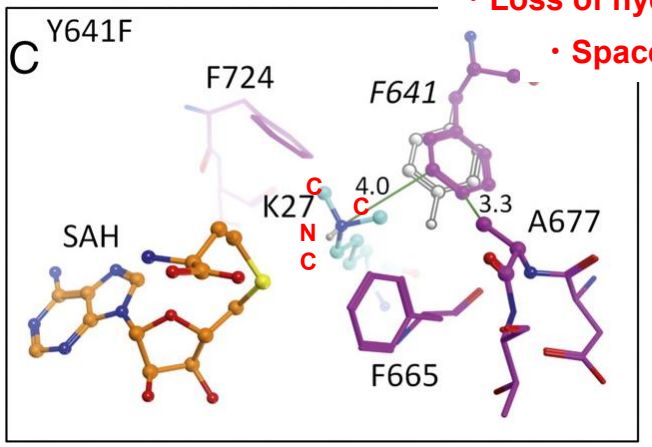

Y641 and A677G EZH2 mutations alter the lysine binding pocket to affect H3K27 substrate specificity. A homology model of WT EZH2 was generated using the crystal structure of GLP/EHMT1 bound to an H3K9me2 peptide substrate as described in *SI Materials and Methods*. Modeled structures of the active site region in WT (*A*), Y641N (*B*), Y641F (*C*), and A677G (*D*) EZH2 are depicted. For the Y641F and A677G mutant models, the lowest energy rotamer for the 641 residue (F or Y, respectively) was selected after rotating the dimethylated lysine into an orientation optimal for trimethylation. In *C* and *D*, the WT Y641 orientation is shown in a gray outline to highlight the alternative low-energy conformations adopted by the 641 residue in these mutants. Key heavy atom distances (measurement unit = Å) are indicated with green lines. S-adenosyl-homocysteine (SAH) is colored with orange carbons, EZH2 residues are colored with magenta carbons, and the dimethylated H3K27 is colored with cyan carbons.**OPEN IN VIEWER**

McCabe M.T.et al, *Proc. Natl. Acad. Sci. USA*, **2012**, *109*, 2989.

EZH2 (H3K27 methyltransferase)

- **EZH2 (WT) and EZH2 (Mutant) prefer different methylation reactions.**

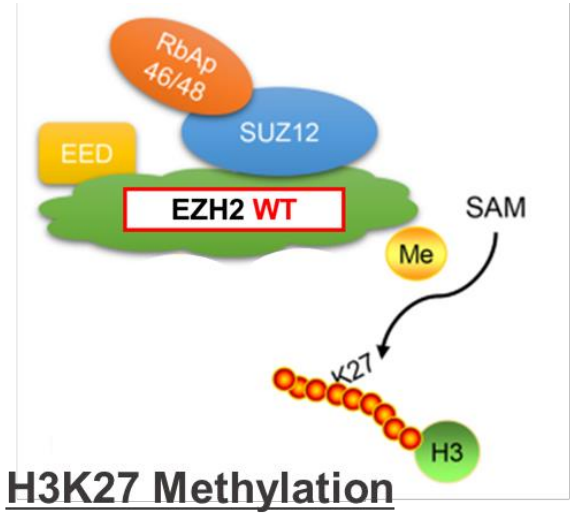

H3K27 Methylation

EZH2 (WT)
◎Me0→Me1
○Me1→Me2
△Me2→Me3

Overexpression of WT ➡ Me3 accumulation

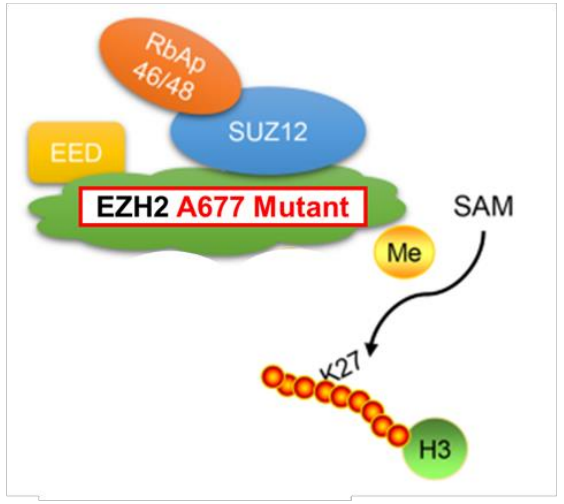

EZH2 (A677 Mut)
○Me0→Me1
○Me1→Me2
○Me2→Me3⚠

Me3 accumulation

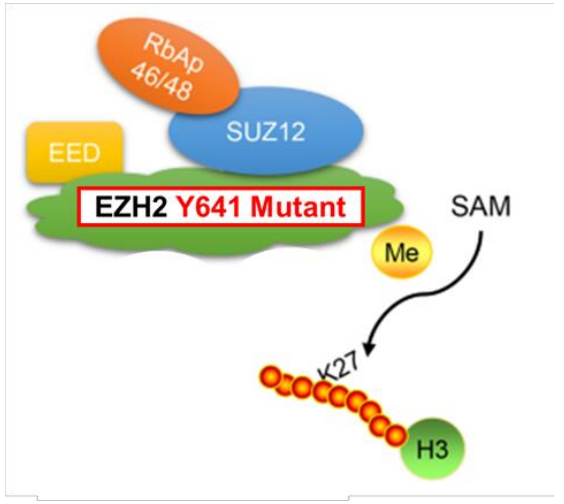

EZH2 (Y641 Mut)
△Me0→Me1
△Me1→Me2
◎Me2→Me3⚠

Cooperation with WT ➡Me3 accumulation

Gene silencing
➡ Cancers

McCabe M.T.et al, *Proc. Natl. Acad. Sci. USA,* **2012**, *109*, 2989.
An, R., Li, YQ., Lin, YL. *et al, Cancer Gene Ther*, **2022**

EZH2 (H3K27 methyltransferase)

- **H3K27Me3 is associated with disease.**

• H3K27Me3 levels in cancer cell lines

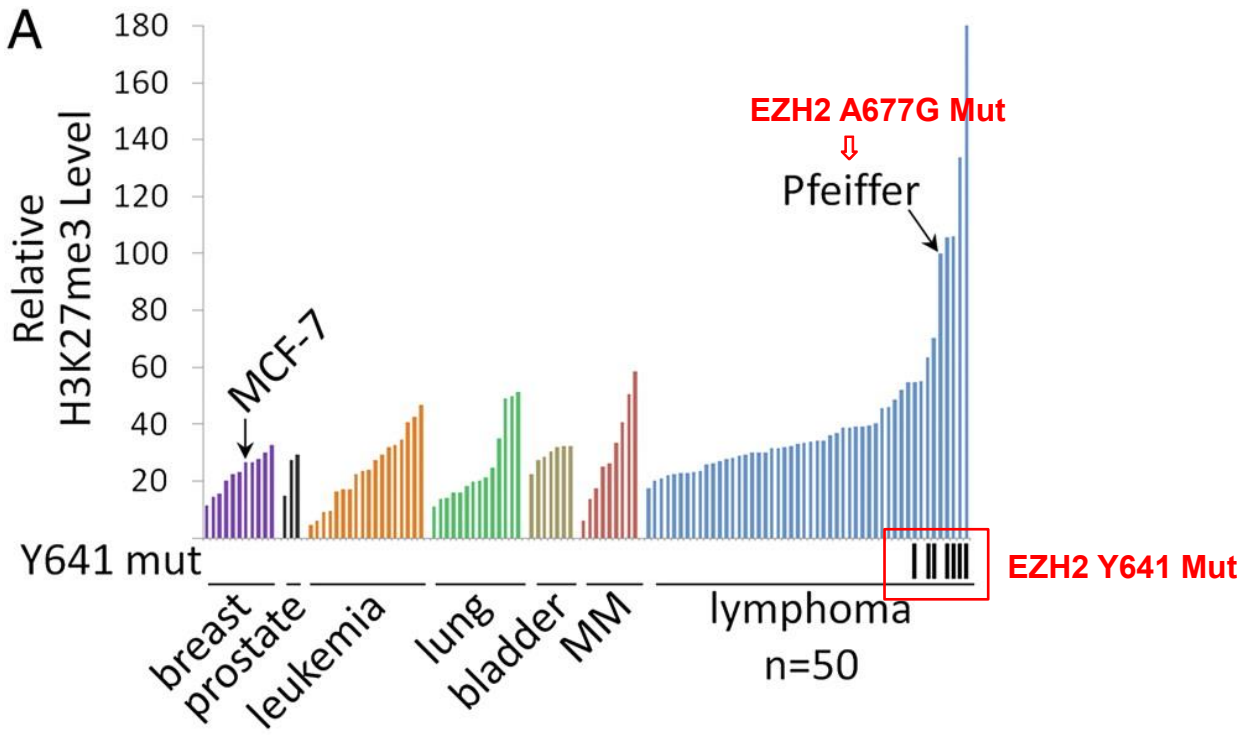

• H3K27Me3 levels in WT and Mut EZH2 cell lines

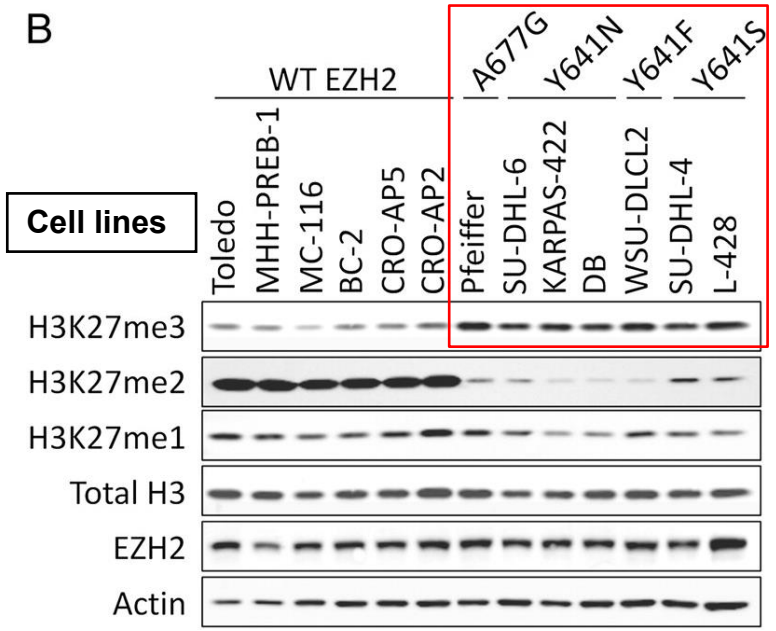

➡ Lymphoma cells express mutant EZH2 and have high H3K27Me3 levels.

A subset of lymphoma cell lines exhibits elevated H3K27me3 levels. (A) Global H3K27me3 levels (normalized to total H3) were determined for 111 cancer cell lines from seven different cancer types using H3K27me3 and total H3 ELISAs. Lymphoma cell lines harboring heterozygous Y641 mutations are indicated by black tick marks below the graph. MM, multiple myeloma. (B) Western blot analysis was performed with antibodies specific for H3K27me3, H3K27me2, H3K27me1, total histone H3, EZH2, and actin using protein lysates from a panel of lymphoma cell lines. Actin serves as a loading control. EZH2 mutation status as determined from full-length Sanger sequencing is indicated.

McCabe M.T.et al, *Proc. Natl. Acad. Sci. USA,* **2012**, *109*, 2989.

Short summary

- EZH2 methylates H3K27.

- EZH2 mutants (A677, Y641) accumulate H3K27Me3.

H3K27 Methylation

EZH2 (WT)	EZH2 (A677 Mut)	EZH2 (Y641 Mut)
◎Me0→Me1	○Me0→Me1	△Me0→Me1
○Me1→Me2	○Me1→Me2 ⚠	△Me1→Me2 ⚠
△Me2→Me3	○Me2→Me3	◎Me2→Me3

This difference is due to hydrogen bonds and wide space.

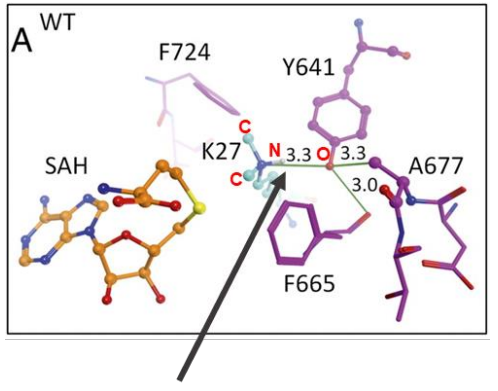

- H3K27Me3 is highly expressed in lymphoma cells.

➡ EZH2 Mutations (A677 or Y641) were identified. ⋯⋯▸ **EZH2 Inhibitors**

Contents

EZH2 inhibitors ①EPZ005687

- **High-throughput screening of a 175,000-compound subset against recombinant WT PRC2 Complex.**

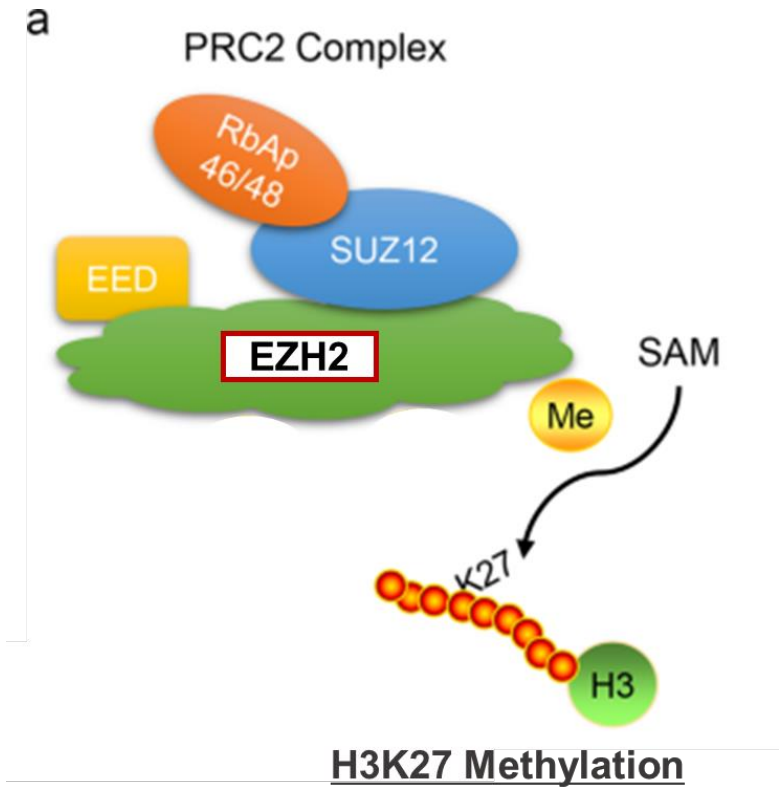

H3K27 Methylation

EZH2 Inhibitor

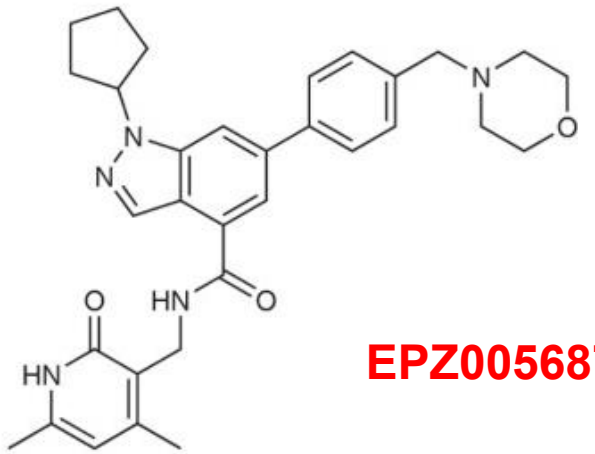

EPZ005687

EPZ005687 (**4**)
PRC2 K_i = 24 nM

Knutson, S et al, *Nat Chem Biol*, **2012**, *8*, 890.

EZH2 inhibitors ①EPZ005687

□ Biochemical characterization of EPZ005687

・Inhibition of EZH2 by EPZ005687 (In the presence of SAM)

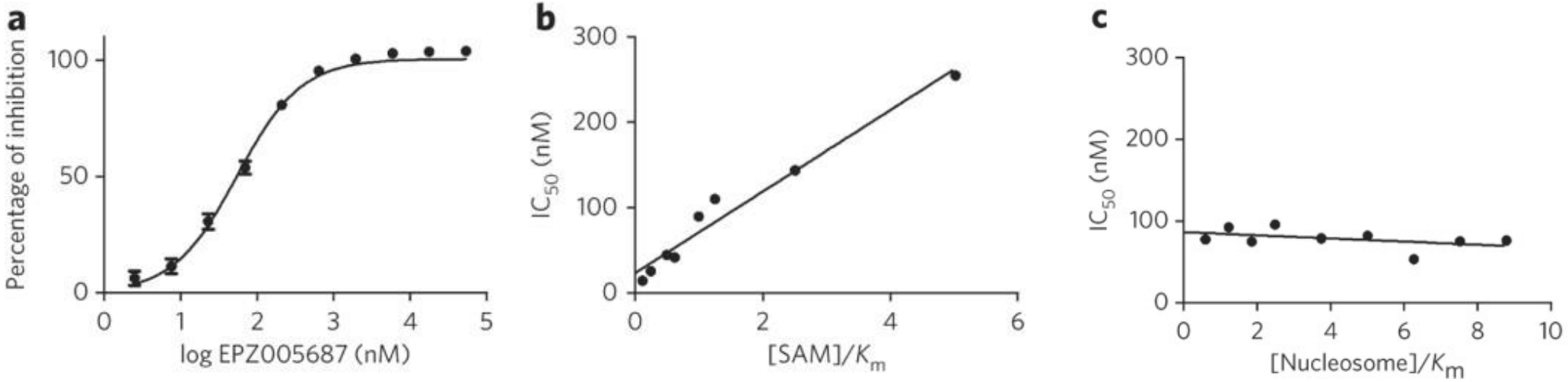

EPZ005687 was competitive with SAM and noncompetitive with Nucleosome.

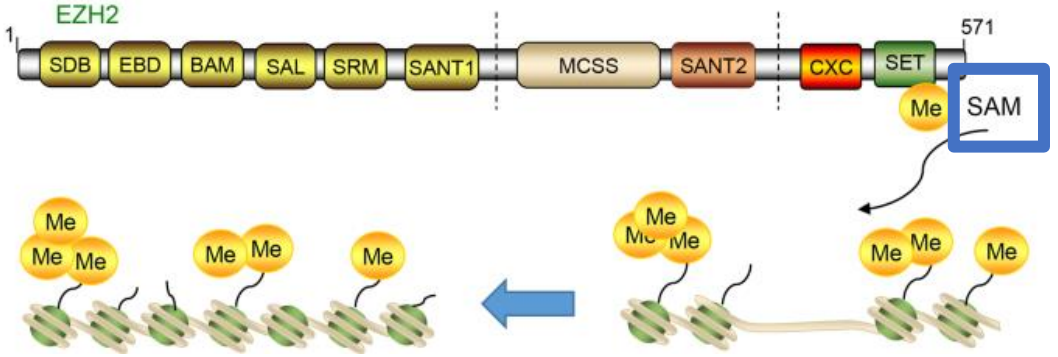

(**a**) Inhibition of EZH2 when activity is assessed under balanced conditions[24] for both SAM and peptide substrates using a Flashplate assay to measure the transfer of a tritiated methyl group from SAM to the peptide. The data are fit to a standard Langmuir isotherm for inhibition, and the IC_{50} of EPZ005687 was calculated to be 54 ± 5 nM with a Hill slope of 1. The data shown are the average and s.d. of seven independent duplicate runs. (**b**) Plot of IC_{50} values of EPZ005687 as a function of SAM concentration relative to the K_m of SAM ([SAM]/K_m) measured using a Flashplate assay similar to the IC_{50} measurements described above. These values show a linear relationship, as expected for SAM-competitive inhibition with a K_i of 24 ± 7 nM (± s.d. of three experiments). (**c**) Plot of IC_{50} values of EPZ005687 as a function of chicken erythrocyte oligonucleosome concentration relative to the K_m of nucleosome ([Nucleosome]/K_m) measured using a filter-binding microplate assay to measure the transfer of tritiated methyl groups from SAM to the oligonucleosome. As expected for a noncompetitive inhibitor with respect to this substrate, the IC_{50} is unaffected as the concentration of oligonucleosome is increased. The mean and standard error of three experiments are shown.

Knutson, S et al, *Nat Chem Biol*, **2012**, *8*, 890.
An, R., Li, YQ., Lin, YL. *et al, Cancer Gene Ther*, **2022**

EZH2 inhibitor ①EPZ005687

▫ Biochemical characterization of EPZ005687

・ Affinity map with methyltransferases

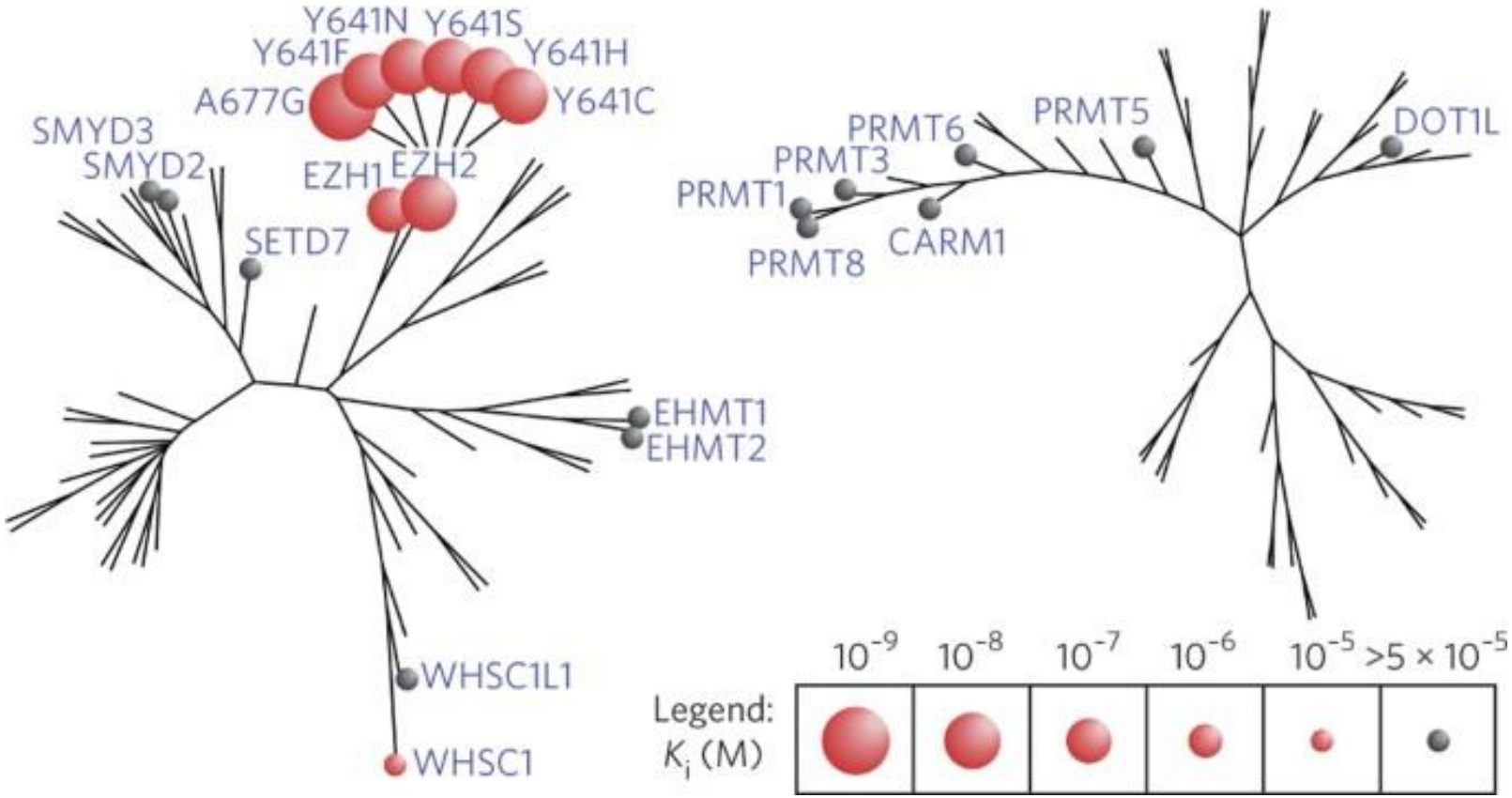

Figure 3: Ligand affinity maps of EPZ005687 across the family trees of human lysine methyltransferases and arginine methyltransferase enzymes show EPZ005687 is a selective and potent inhibitor of EZH2 and EZH1 enzymes. The K_i of EPZ005687 was measured across a panel of recombinant lysine methyltransferase (KMT; left) and arginine methyltransferase (RMT; right) enzymes at balanced conditions[24] of both the SAM and peptide or protein substrates. The EZH2 Tyr641 and Ala677 mutant enzymes are indicated above wild-type EZH2. The K_i values were converted to pK_i values and used to generate red circles of proportional sizes to indicate the extent of inhibition as shown in the legend. Larger circles correlate to increased potency versus the enzymes, and gray circles indicate that inhibition was not measurable at concentrations up to 50 μM of EPZ005687.

➡ EPZ005687 can selectively inhibit WT and Mutant EZH2.

Knutson, S et al, *Nat Chem Biol*, **2012**, *8*, 890.

EZH2 inhibitor ①EPZ005687

□ Ability of EPZ005687 in lymphoma cells

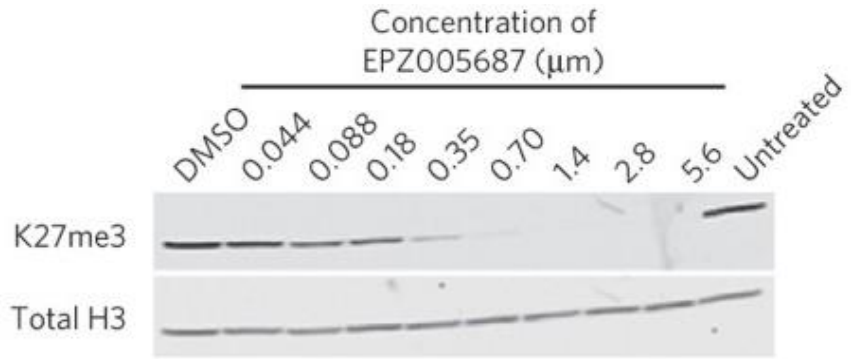

(EZH2 WT lymphoma cell OCI-LY19 + EPZ005687)

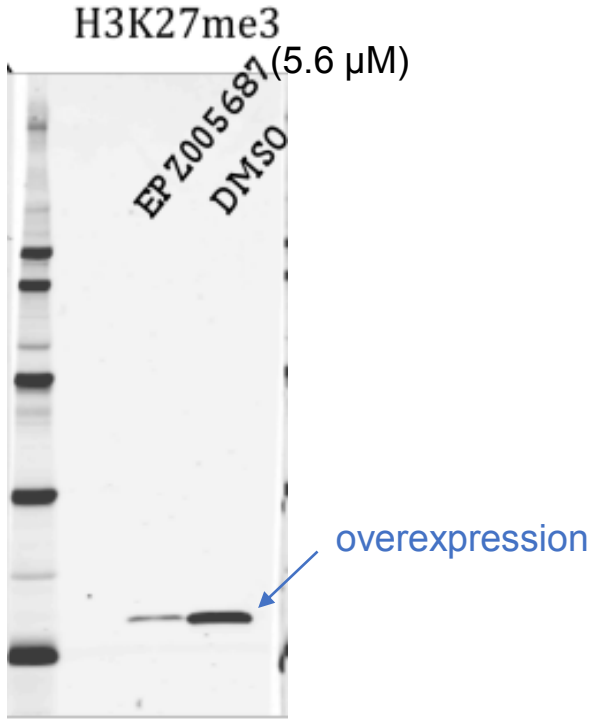

(EZH2 Mutant lymphoma cell WSU-DLCL2 + EPZ005687)

➡ EPZ005687 reduces H3K27Me3 expressed in WT and Mutant EZH2 cells.

(**a**) The wild-type EZH2 lymphoma cell line OCI-LY19 shows a dose-dependent decrease in H3K27me3 after treatment with EPZ005687 for 96 h. (**b**,**c**) A wild-type lymphoma cell line, OCI-LY19 (**b**), and a mutant lymphoma cell line, WSU-DLCL2 (**c**), show the specificity of H3K27 methylation inhibition by EPZ005687 across a broad panel of histone methylation marks. Quantification of methylation changes is represented in the bar graphs to the right of each panel of western blots. Representative western blots (*n* = 1) were normalized to corresponding total H3 and expressed as percent change in EPZ005687-treated versus DMSO-treated cells.

Knutson, S et al, *Nat Chem Biol*, **2012**, *8*, 890.

EZH2 inhibitor ①EPZ005687

□ Ability of EPZ005687 in lymphoma cells

(Previous Slide) EPZ005687 reduces H3K27Me3 expressed in WT and Mutant EZH2 cells.

・Effect on cell proliferation

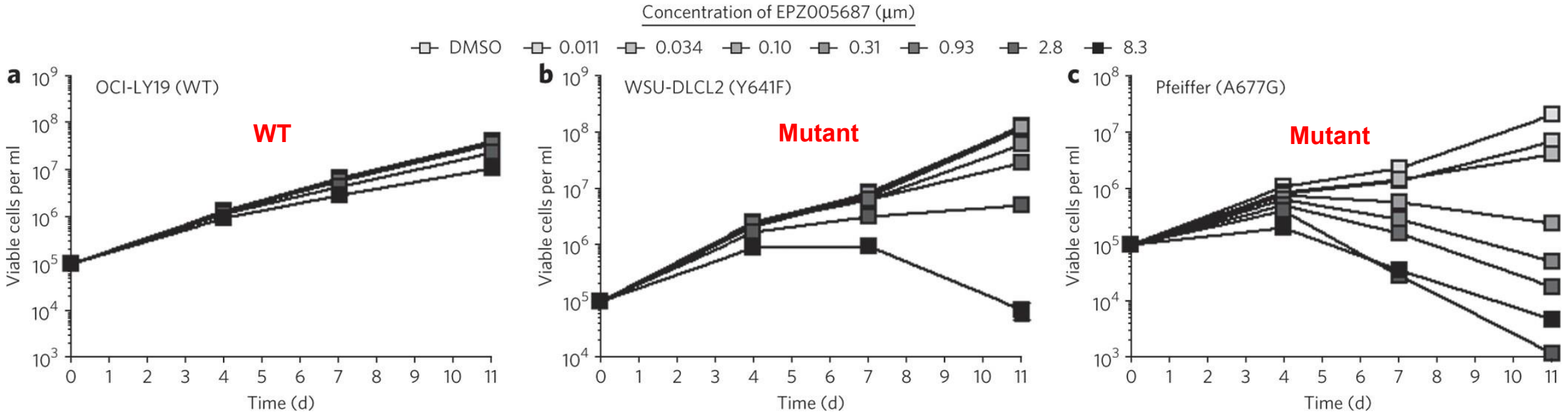

➡ EPZ005687 is effective against cell proliferation caused by Mutant EZH2.

Knutson, S et al, *Nat Chem Biol*, **2012**, *8*, 890.

Short summary

- EZH2 inhibitor : EPZ005687

- Competes with SAM (=methyl donor).

- Selectively inhibits EZH2 WT and Mutant.

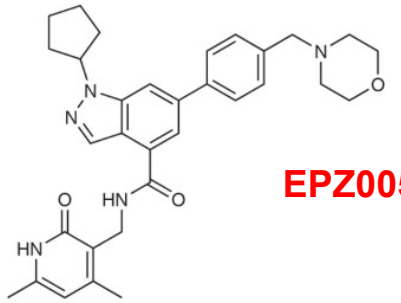

EPZ005687

EZH2 WT cell — ○ →

EZH2 Mutant cell — ○ →

(H3K27Me3 is overexpressed.)

EPZ005687

H3K27Me3 expression is reduced.

— ? × →

— ○ →

Cell proliferation is inhibited.

? → Hypothesis

EZH2 WT cell : H3K27Me3 ↑ ····→ Cell proliferation ←— Other factors

EZH2 Mutant cell : H3K27Me3 ↑ ——→ Cell proliferation

Knutson, S et al, *Nat Chem Biol*, **2012**, *8*, 890.

EZH2 inhibitor ①EPZ005687

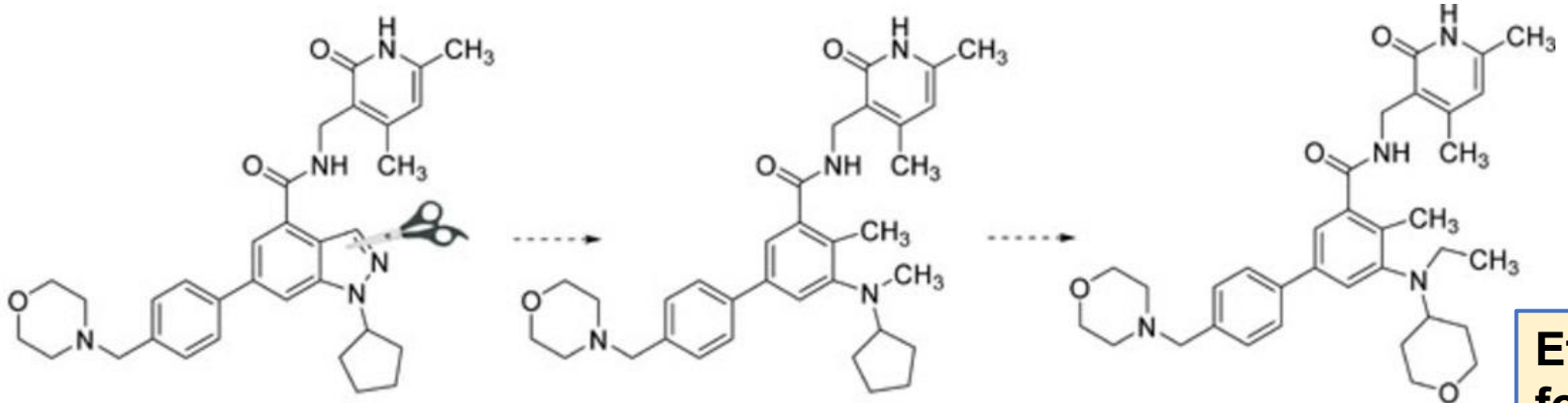

EPZ005687

EPZ-6438
(tazemetostat)

Effective in EZH2 mutation-positive follicular lymphoma.
Approved in Japan in June 2021.

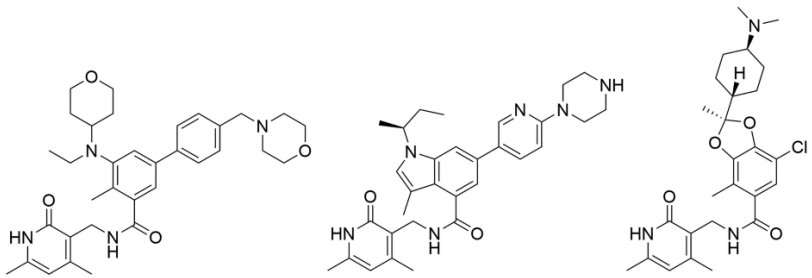

1 (EPZ-6438/Tazemetostat)　2 (GSK-126)　3 (DS-3201b)

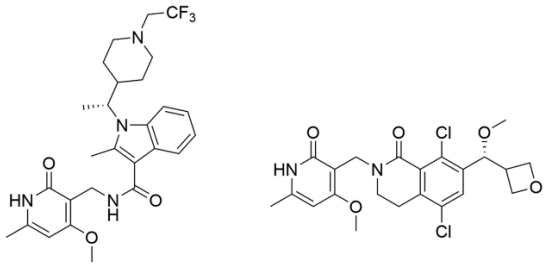

4 (CPI-1205)　5 (PF-06821497)

Research on diverse EZH2 inhibitors is ongoing.

(Next)
New EZH2 inhibitors recently developed will be discussed.

S. K. Knutson et al, *Proc. Natl. Acad. Sci. USA* **2013**,*110*,7922.

Bin Zhou et al, *J. Med. Chem.* **2021**, *64*, 15170.

EZH2 inhibitor ② IHMT-EZH2-115

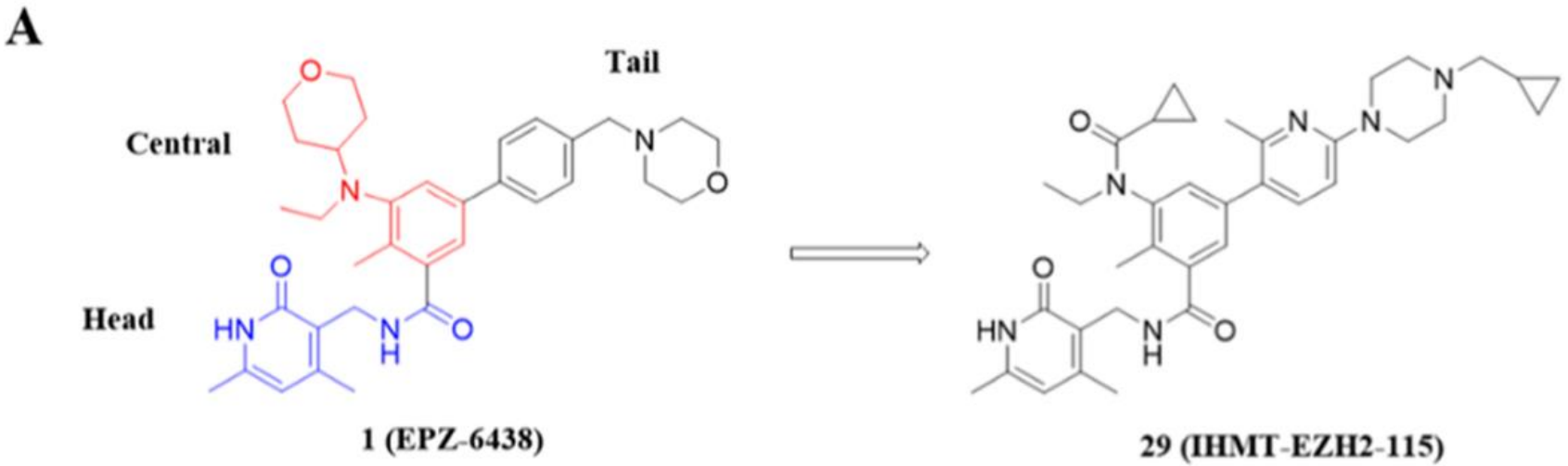

Bin Zhou et al, *J. Med. Chem*. **2021**, *64*, 15170.

EZH2 inhibitor ② IHMT-EZH2-115

▫ **EPZ6438 was docked into the EZH2 crystal structure.**

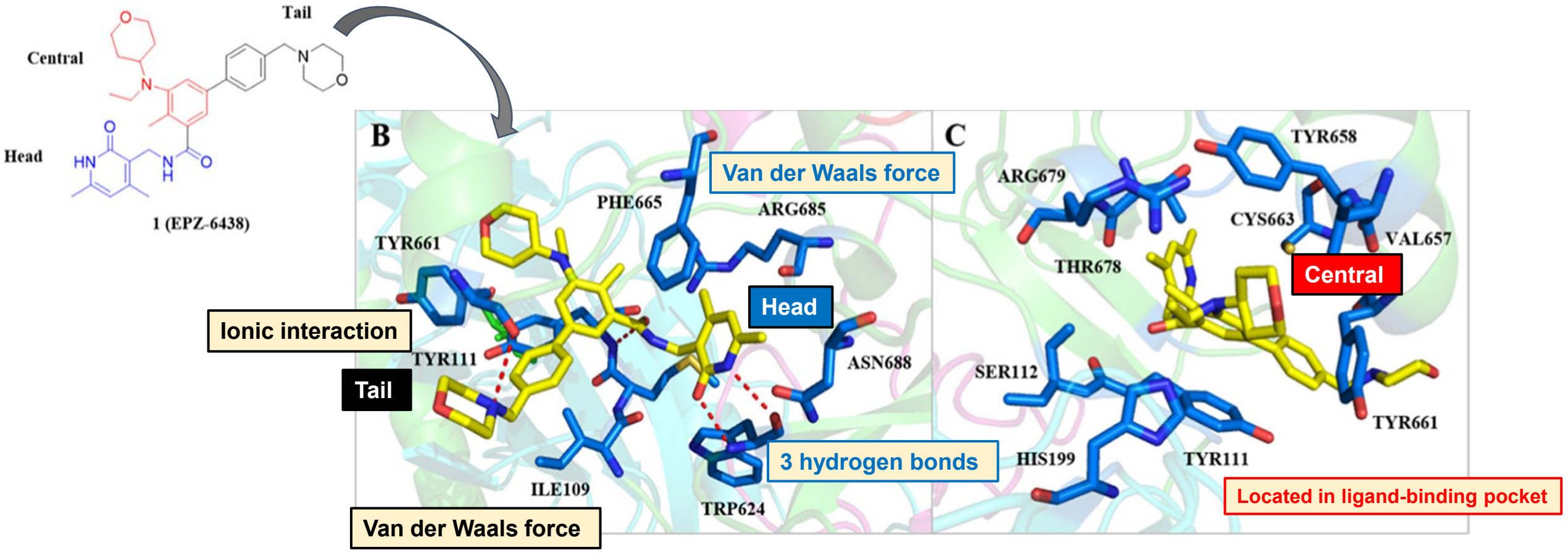

Figure 2. (A) Schematic illustration of the discovery of **29**. (B) and (C) Binding modes of **1** with PRC2 (PDB: 5IJ7). **1** was labeled in color by atoms (carbon in yellow, nitrogen in blue, and oxygen in red). The hydrogen bonds were labeled as red dashed lines. The key amino acid residues for binding were labeled as follows: carbon in marine, nitrogen in blue, and oxygen in red.

Bin Zhou et al, *J. Med. Chem.* **2021**, *64*, 15170.

EZH2 inhibitor ③IHMT-EZH2-115

□ Central Structure Optimization

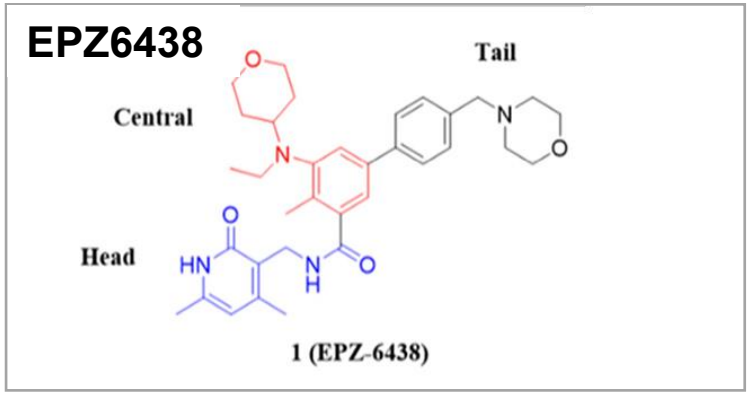

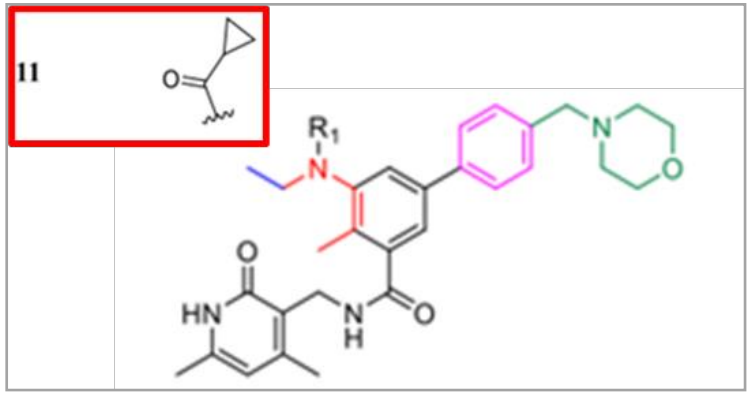

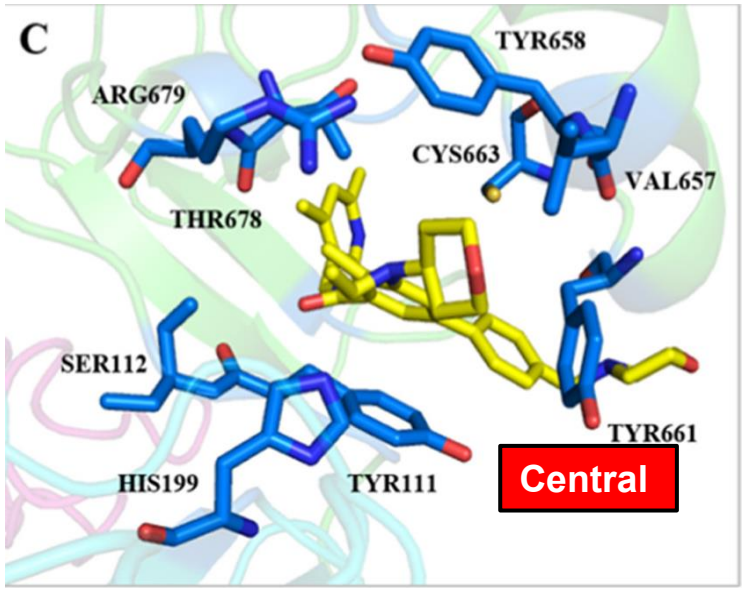

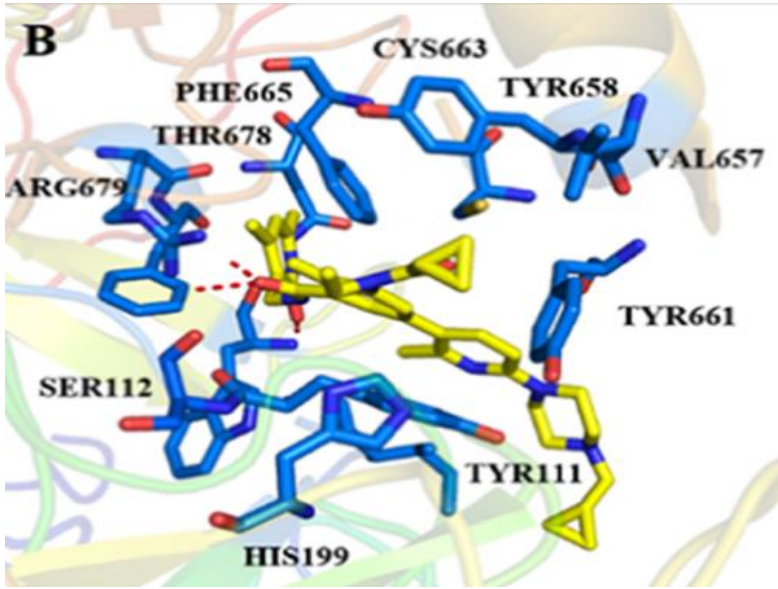

Hydrogen bonds could be formed.

Compd.	R_1	EZH2 WT (IC_{50}: nM)	EZH2-Y641F (IC_{50}: nM)	WSU-DLCL2 (GI_{50}: μM)
1	/	11[21]	N/A	0.3 ± 0.1
6	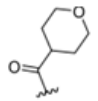	33.7 ± 1.5	268.9 ± 37.6	16.2 ± 3.9
7	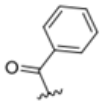	371 ± 80	3174 ± 487	34.7 ± 22.9
8	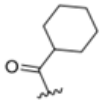	198.7 ± 62.4	1057 ± 26	32.4 ± 0.3
9	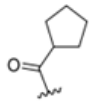	18.2 ± 1.9	64.0 ± 5.3	0.3 ± 0.1
10		47.7 ± 15.2	102 ± 2	0.9 ± 0.2
11		16.8 ± 5.3	49.3 ± 2.6	0.2 ± 0.1
12	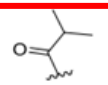	25.1 ± 2.3	56.6 ± 4.3	0.5 ± 0.2
13		51.7 ± 6.8	97.4 ± 0.9	0.9 ± 0.1
14	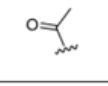	17.5 ± 2	73.8 ± 4.1	1.3 ± 0.1

Bin Zhou et al, *J. Med. Chem.* **2021**, *64*, 15170.

EZH2 inhibitor ③IHMT-EZH2-115

▫ Tail Structure Optimization

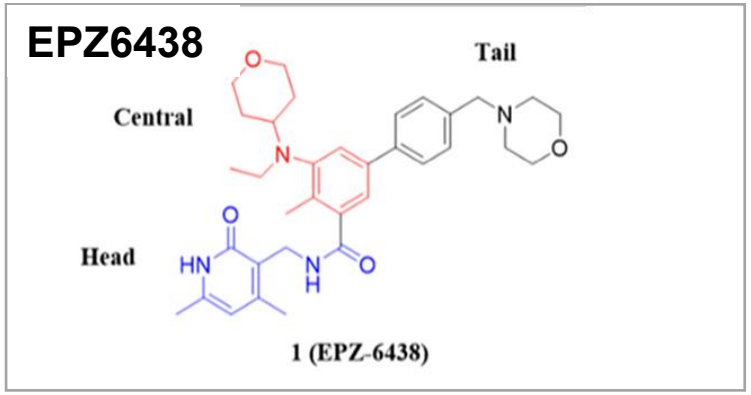

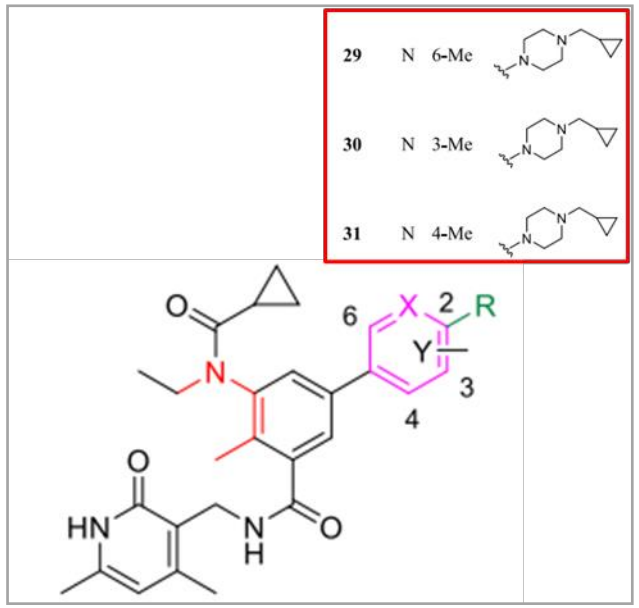

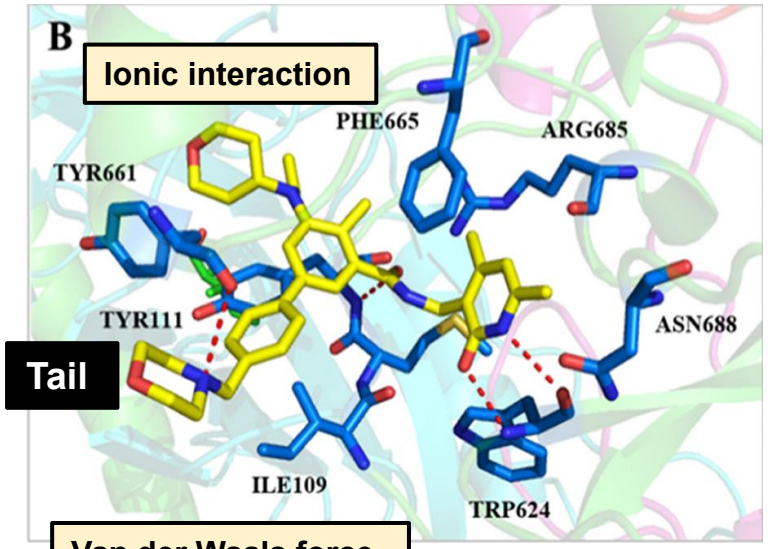

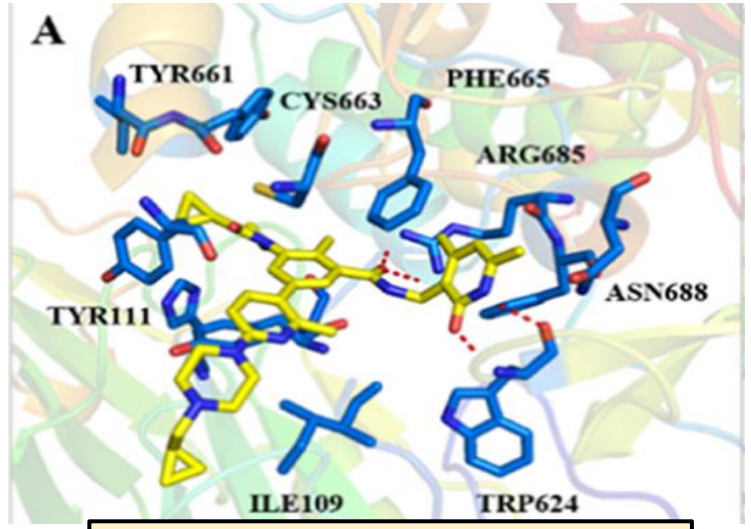

Compd.	X	Y	R	EZH2 WT (IC_{50}: nM)	EZH2-Y641F (IC_{50}: nM)	WSU-DLCL2 (GI_{50}: μM)
19	-	-	NH_2	19.1± 0.3	61.2 ± 1.7	0.8 ± 0.1
20	-	-	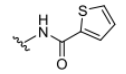	47.3 ± 5.3	150.3 ± 1.1	0.9 ± 0.3
21	-	-	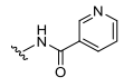	40.7 ± 4.3	70.3 ± 2.7	0.8 ± 0.1
22	-	-	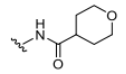	33.7 ± 1.3	49.6 ± 1.4	0.7 ± 0.4
23	-	-	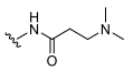	11.7 ± 0.1	34.9 ± 0	1.8 ± 0.4
24	-	-	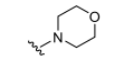	37.6 ± 3.8	79.1 ± 3.3	0.2 ± 0.1
25	-	-	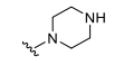	15.1 ± 0.9	33.1 ± 2.1	0.2 ± 0.1
26	-	-	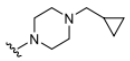	25.3 ± 0.6	50.5 ± 6.2	0.1 ± 0.1
27	-	-	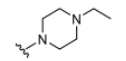	16.0 ± 1.6	40.7 ± 3.3	0.2 ± 0.1
28	N	-	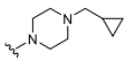	10.1 ± 0.7	24.4 ± 2.6	0.2 ± 0.1
29	N	6-Me	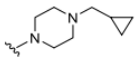	26.1 ± 1.3	72.3 ± 1.9	0.2 ± 0.1
30	N	3-Me	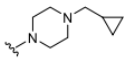	12.0 ± 1.5	30.4 ± 0.8	0.3 ± 0.1
31	N	4-Me	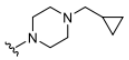	16.7 ± 1.2	40.4 ± 0.4	0.2 ± 0.1

Bin Zhou et al, *J. Med. Chem.* **2021**, *64*, 15170.

▫ **Optimization complete**

➡ **Pharmacokinetic characterization in rats.**

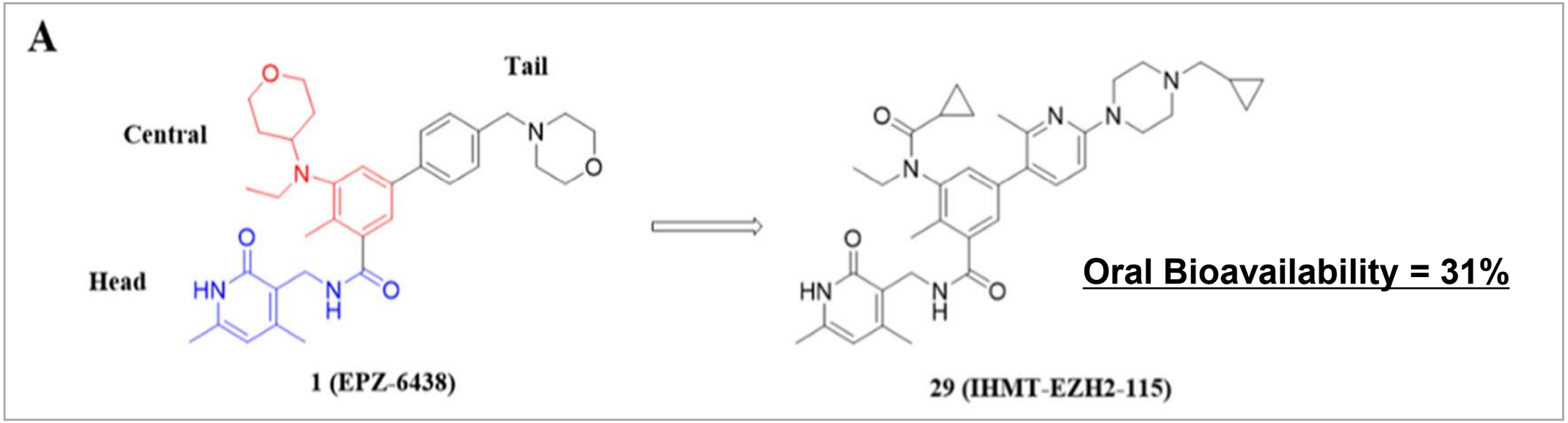

EZH2 inhibitor ③IHMT-EZH2-115

- 1(EPZ6438) vs 29(IHMT-EZH2-115)

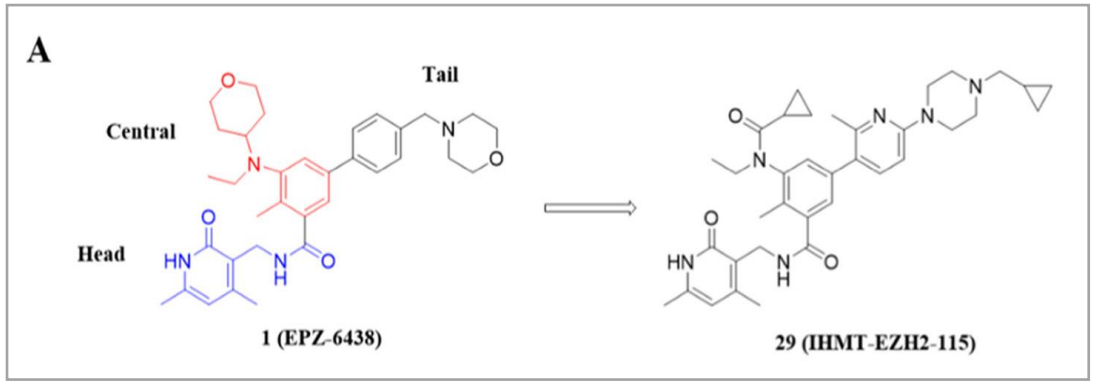

Table 6. H3K27 Trimethylation Inhibition in Lymphoma Cell Lines by 29

cell	EC_{50} (nM)	
	compd. **29**	compd. **1**
U2932 (EZH2 WT)	42	46
Raji (EZH2 WT)	13	46
Daudi (EZH2 WT)	19	51
Pfeiffer (EZH2 A677G)	1.5	6
WSU-DLCL2 (EZH2 Y641F)	27	5
Karpas-422 (EZH2 Y641N)	20	64
SU-DHL-6 (EZH2 Y641N)	34	62
SU-DHL-4 (EZH2 Y641S)	21	64

➡ 29 can strongly inhibit trimethylation.

Table 7. Antiproliferative Effects of 29 against a Panel of Lymphoma Cell Lines[a]

cell	GI_{50} (μM)	
	compd. **29**	compd. **1**
Pfeiffer (EZH2 A677G)	0.003 ± 0.001	0.002 ± 0.001
WSU-DLCL2 (EZH2 Y641F)	0.14 ± 0.08	0.08 ± 0.04
Karpas-422 (EZH2 Y641N)	0.05 ± 0.03	0.09 ± 0.05
SU-DHL-6 (EZH2 Y641N)	1.10 ± 0.56	1.05 ± 0.56
SU-DHL-4 (EZH2 Y641S)	3.87 ± 2.00	3.39 ± 1.71
U2932 (EZH2 WT)	>10	>10
Raji (EZH2 WT)	>10	>10
Daudi (EZH2 WT)	>10	>10

[a]All GI_{50} values were obtained by triplet testing.

➡ 29 can inhibit cell proliferation.
(EZH2 Mutant only)

Bin Zhou et al, *J. Med. Chem.* **2021**, *64*, 15170.

Short summary (previous)

- EZH2 inhibitor : **EPZ005687**

- Competes with SAM (=methyl donor).

- Selectively inhibits EZH2 WT and Mutant.

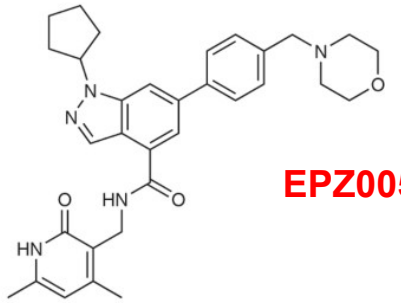

EPZ005687

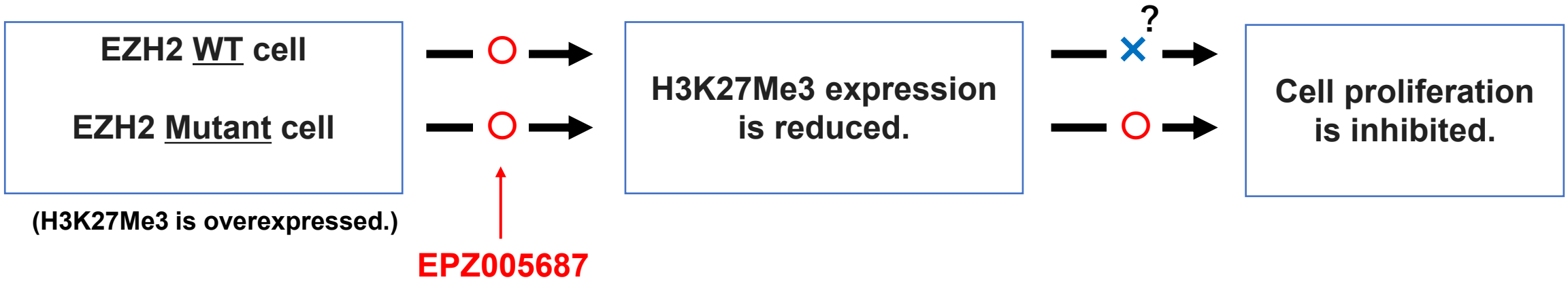

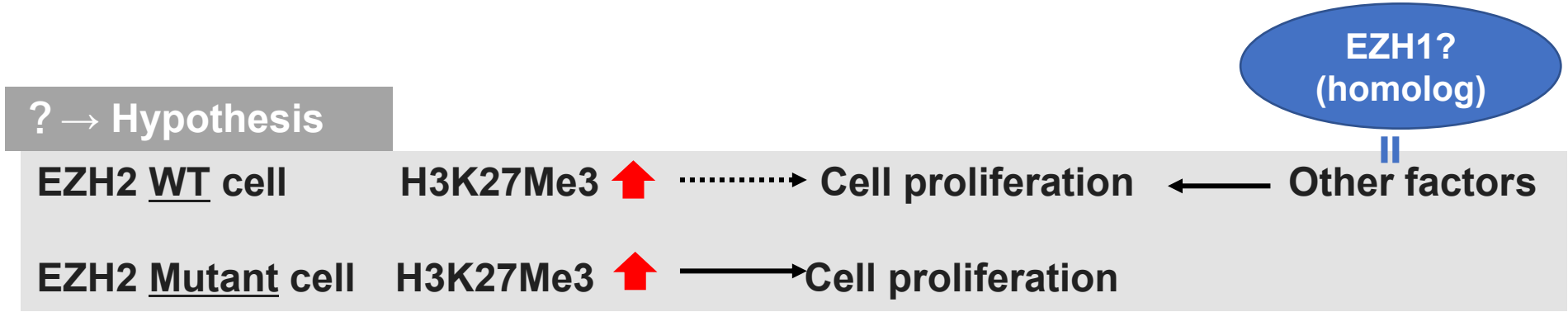

Knutson, S et al, *Nat Chem Biol*, **2012**, *8*, 890.

EZH2 inhibitor ③IHMT-EZH2-115

□ 1(EPZ6438) vs 29(IHMT-EZH2-115)　in vivo

cell	EC_{50} (nM) compd. **29**	compd. **1**
Pfeiffer (EZH2 A677G)	1.5	6
Karpas-422 (EZH2 Y641N)	20	64

cell	GI_{50} (μM) compd. **29**	compd. **1**
Pfeiffer (EZH2 A677G)	0.003 ± 0.001	0.002 ± 0.001
Karpas-422 (EZH2 Y641N)	0.05 ± 0.03	0.09 ± 0.05

・Pfeiffer (EZH2 A677G)

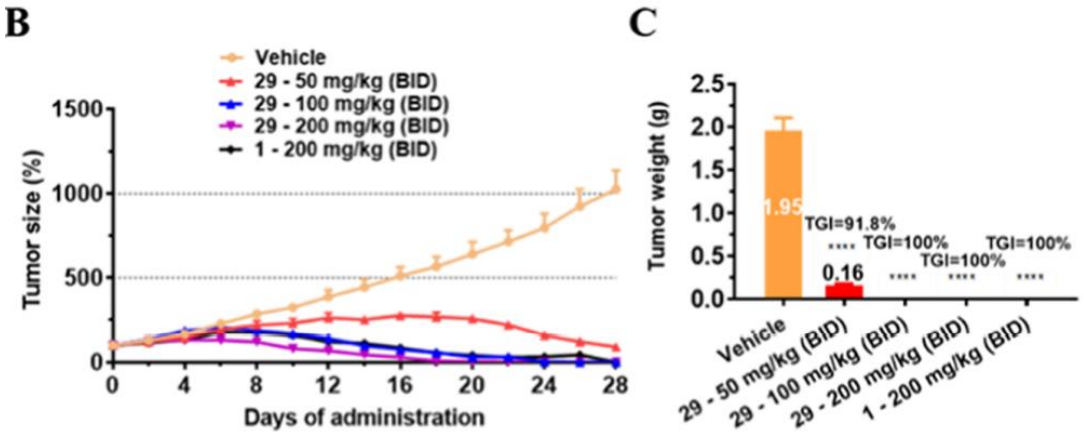

・Karpas-422 (EZH2 Y641N)

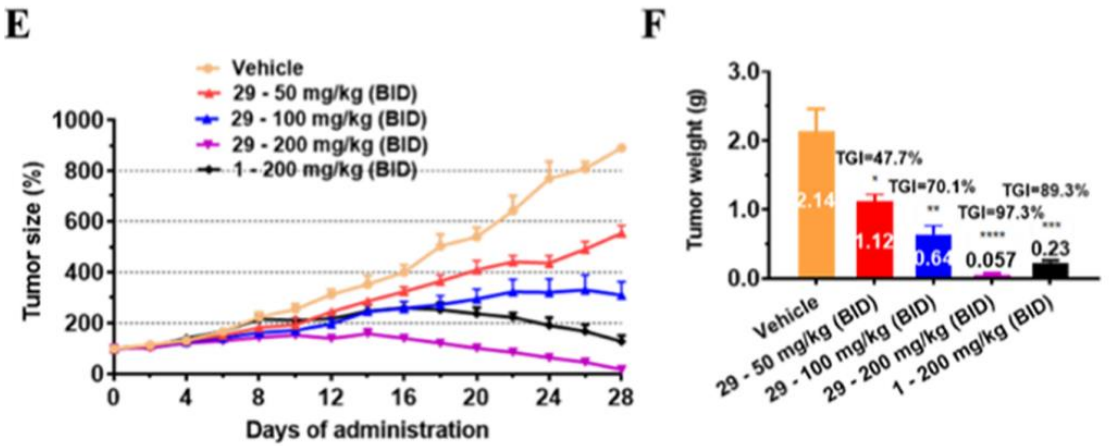

➡ 29 showed a stronger anti-tumor effect than 1.

Bin Zhou et al, *J. Med. Chem.* **2021**, *64*, 15170.

▫ Development of IHMT-EZH2-115

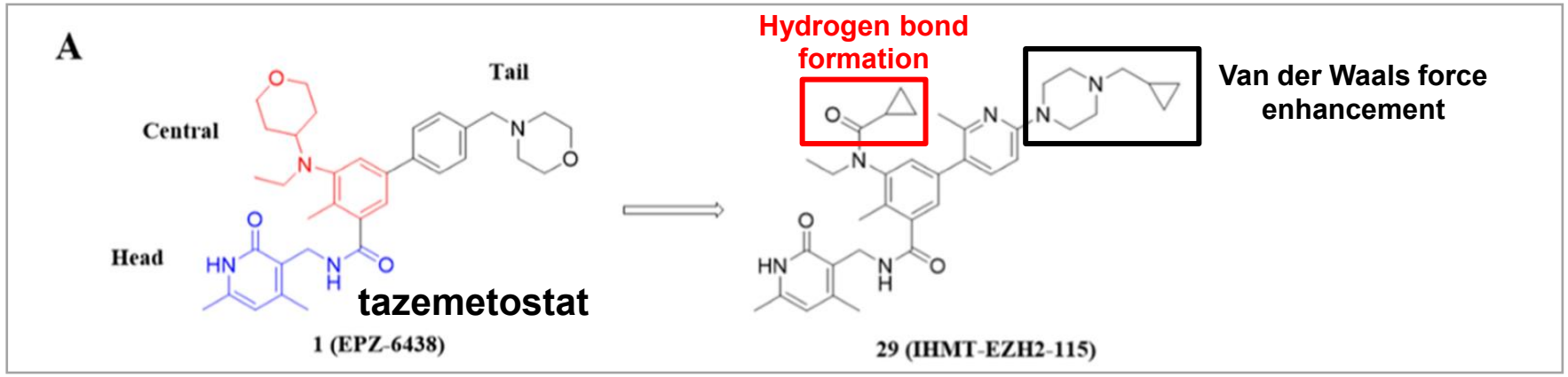

▫ 29 shows excellent antitumor effects in vivo.

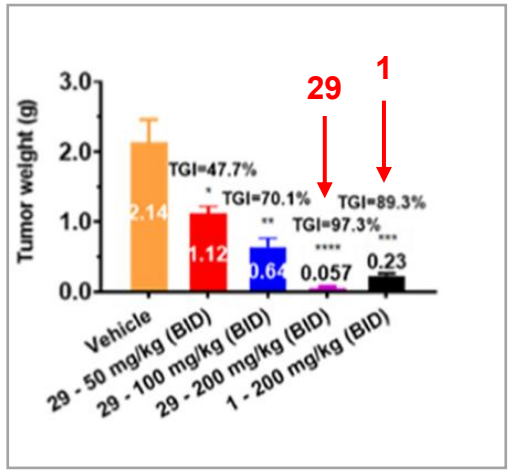

Bin Zhou et al, *J. Med. Chem.* **2021**, *64*, 15170.

Thank you for your attention.

Appendix

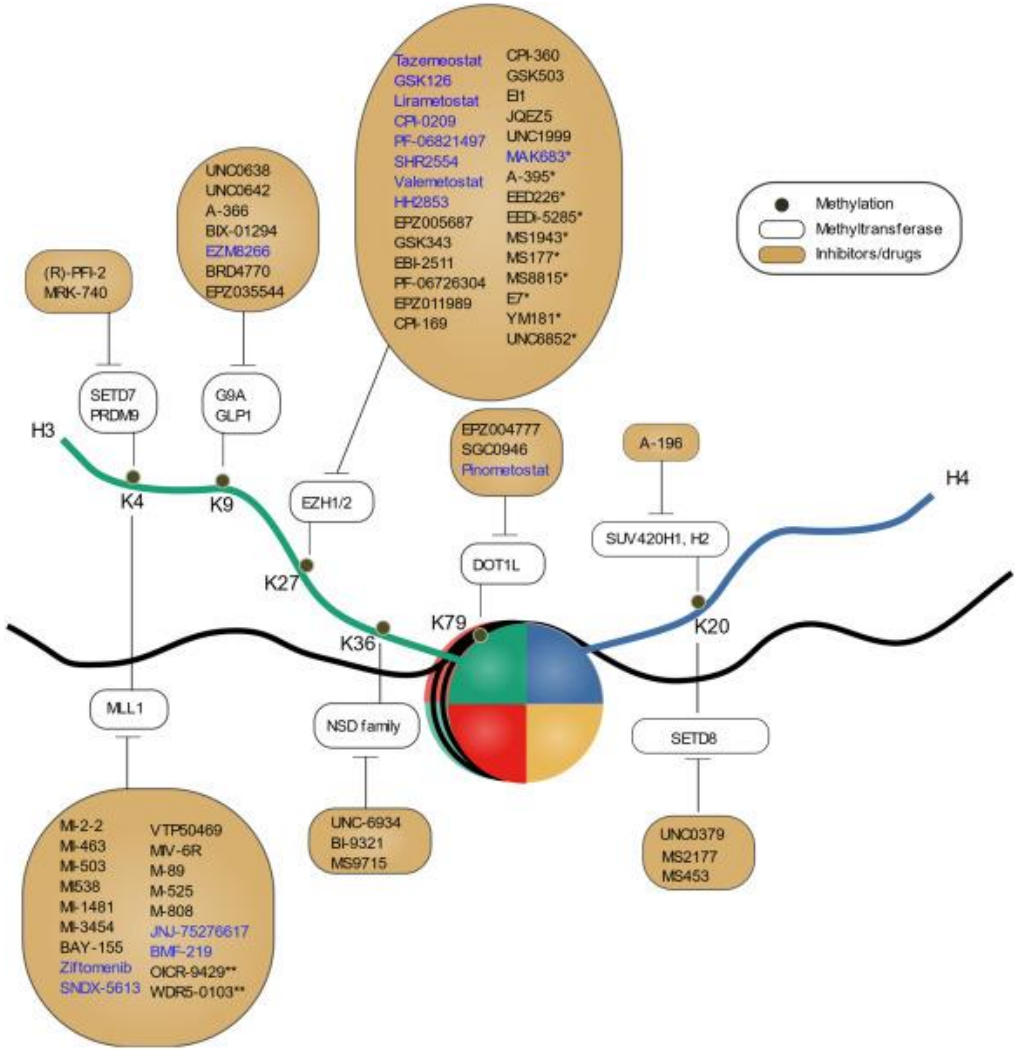
Tazemeostat
GSK126
Lirametostat
CPI-0209
PF-06821497
SHR2554
Valemetostat
HH2853
EPZ005687
GSK343
EBI-2511
PF-06726304
EPZ011989
CPI-169
CPI-360
GSK503
EI1
JQEZ5
UNC1999
MAK683*
A-395*
EED226*
EED-5285*
MS1943*
MS177*
MS8815*
E7*
YM181*
UNC6852*
UNC0638
UNC0642
A-366
BIX-01294
EZM8266
BRD4770
EPZ035544
(R)-PFI-2
MRK-740
Methylation
Methyltransferase
Inhibitors/drugs
SETD7
PRDM9
G9A
GLP1
EZH1/2
EPZ004777
SGC0946
Pinometostat
A-196
SUV420H1, H2
DOT1L
H3
H4
K4
K9
K27
K36
K79
K20
MLL1
NSD family
SETD8
MI-2-2
MI-463
MI-503
MI538
MI-1481
MI-3454
BAY-155
Ziftomenib
SNDX-5613
VTP50469
MIV-6R
M-89
M-525
M-808
JNJ-75276617
BMF-219
OICR-9429**
WDR5-0103**
UNC-6934
BI-9321
MS9715
UNC0379
MS2177
MS453

Appendix

▫ Histone methyltransferase (EZH2)

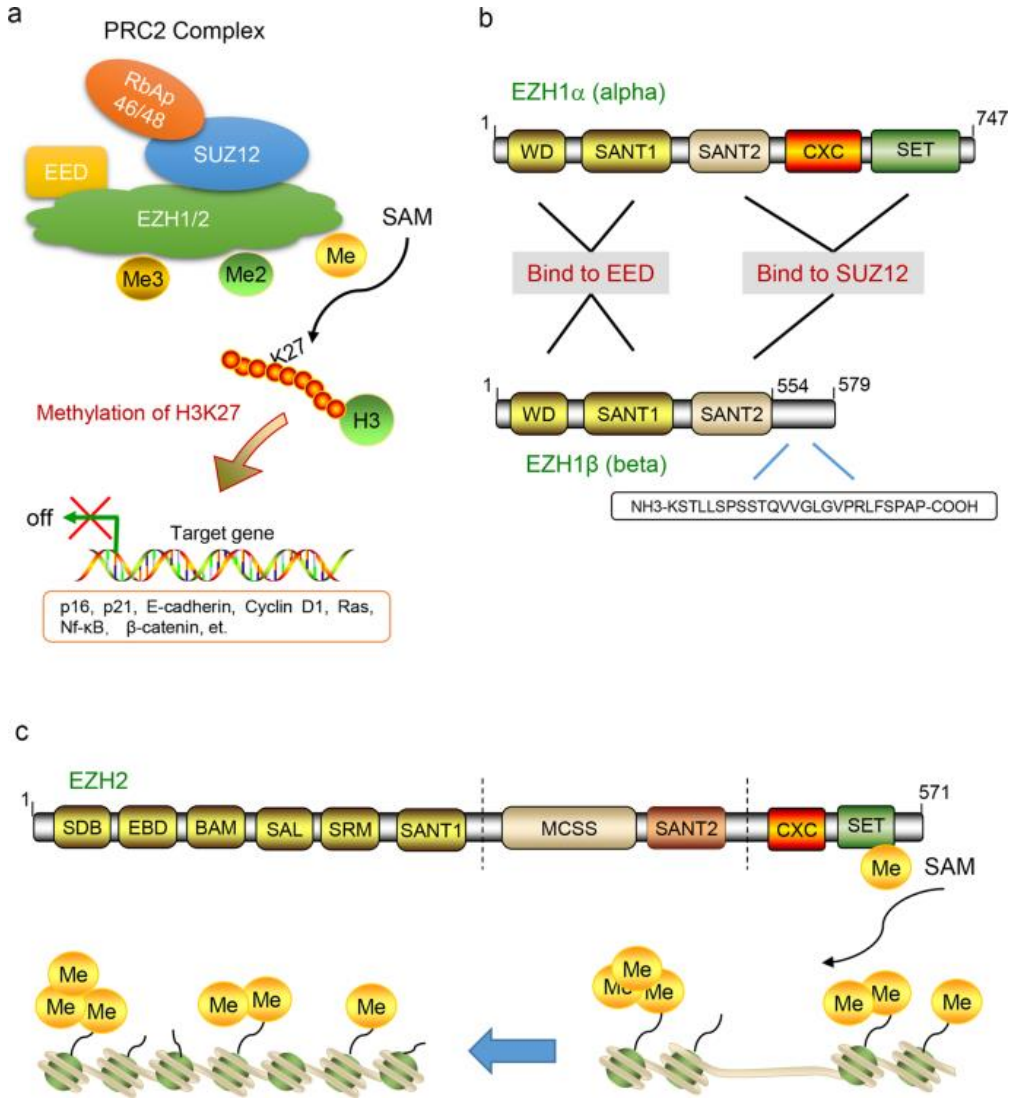

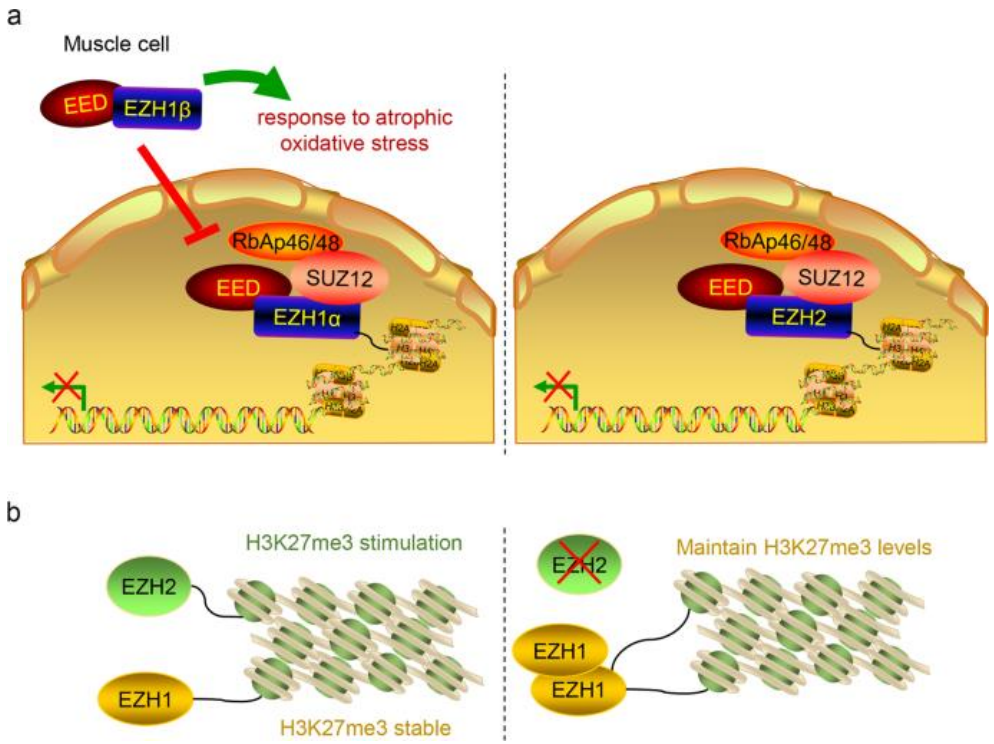

Appendix

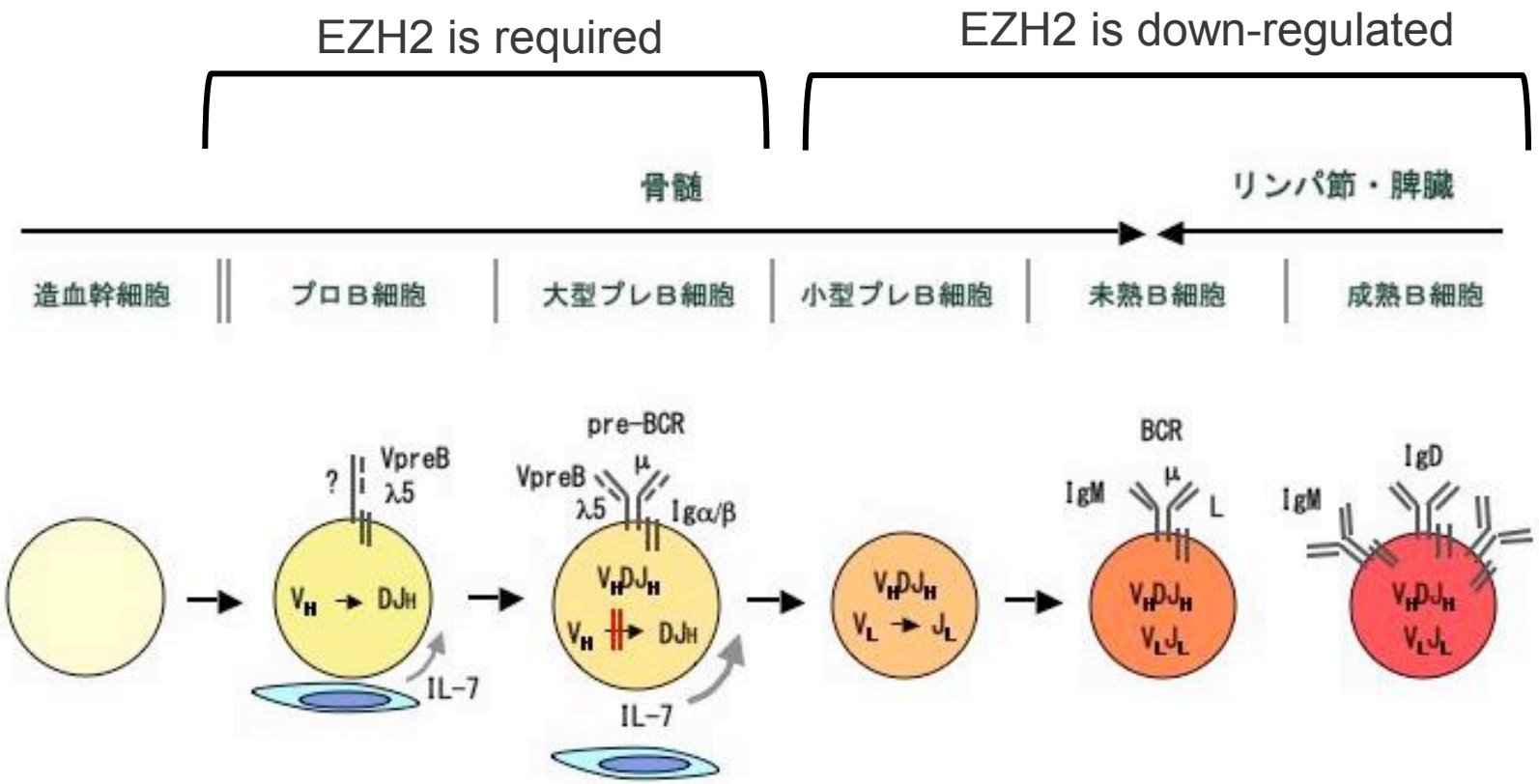
EZH2 is required
EZH2 is down-regulated
骨髄
リンパ節・脾臓
造血幹細胞
プロB細胞
大型プレB細胞
小型プレB細胞
未熟B細胞
成熟B細胞
pre-BCR
VpreB
λ5
Igα/β
IL-7
BCR
IgM
IgD
L

Appendix

□ Differential methylation reactions in WT and Mutant EZH2

H3K27(Me0/Me1/Me2) peptide + EZH2 (WT/Mutant) + SAM

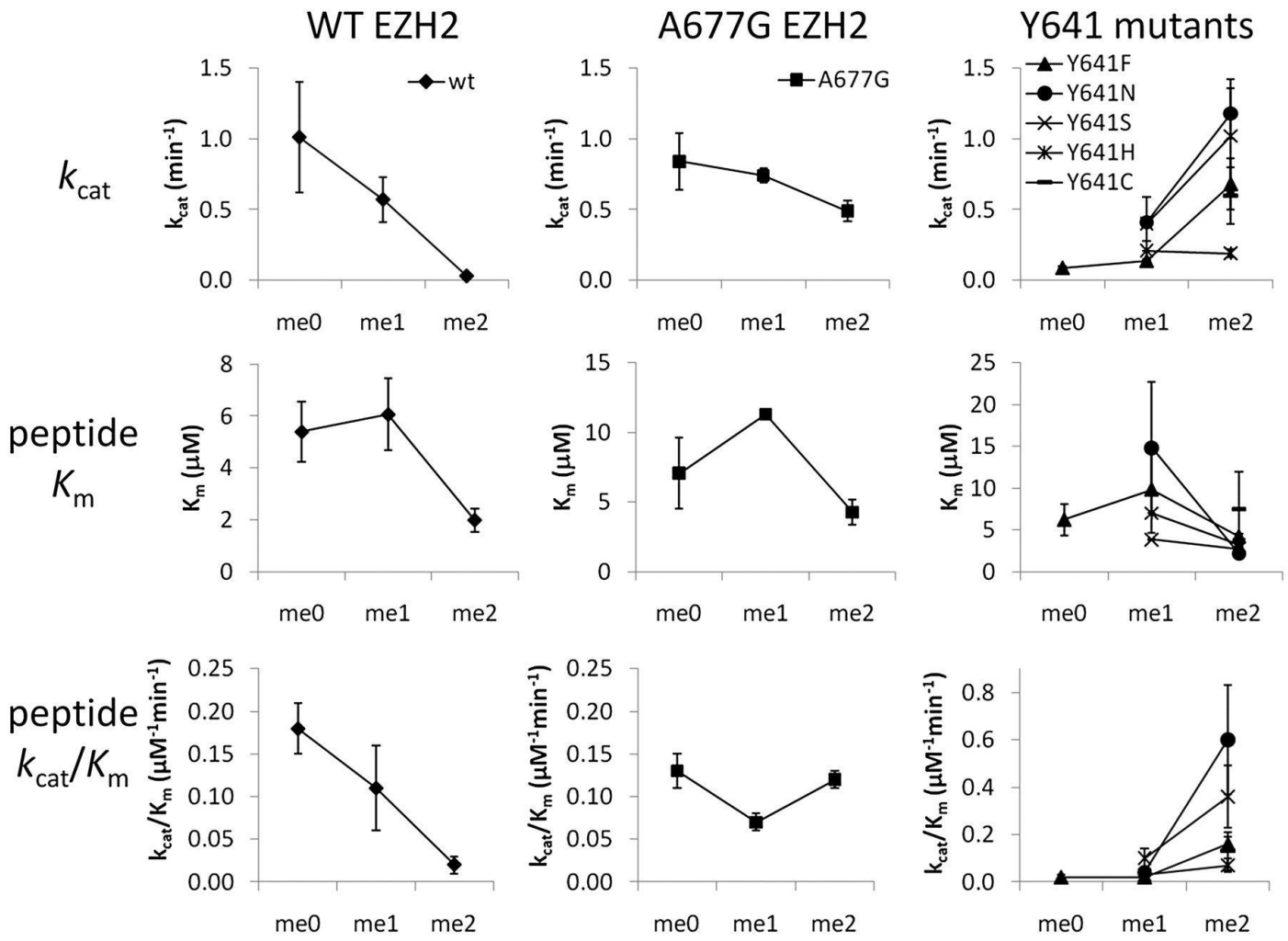

A677G EZH2 mutant exhibits a unique substrate specificity. Enzyme turnover number [k_{cat} (min^{-1})], the substrate concentration at which the reaction rate was half of V_{max} [K_m (μM)], and catalytic efficiency [k_{cat}/K_m ($\mu M^{-1} \cdot min^{-1}$)] were evaluated for recombinant five-member PRC2 complexes containing WT, A677G, or Y641 mutant EZH2 using peptides from histone H3 AA21–44 with no methylation (K27me0), monomethylation (K27me1), or dimethylation (K27me2) at the lysine 27 position. Briefly, EZH2 (20 nM) was combined with varying concentrations of peptide and [^{3}H]-SAM before quenching with unlabeled SAM during the linear portion of their progress curves. Reactions were then captured using filter plates, scintillation mixture was added, and signal was detected with a TopCount liquid scintillation counter (PerkinElmer). Error bars represent the standard deviation from replicate experiments.

EZH2 (WT)	EZH2 (A677 Mut)	EZH2 (Y641 Mut)
◎Me0→Me1	○Me0→Me1	△Me0→Me1
○Me1→Me2	○Me1→Me2	△Me1→Me2
△Me2→Me3	○Me2→Me3	◎Me2→Me3

McCabe M.T.et al, *Proc. Natl. Acad. Sci. USA,* **2012**, *109*, 2989.

Appendix

□ H3K27(Me0/Me1/Me2) peptide + EZH2 (WT/Mutant) + SAM → Activity assessment

• Reaction velocity

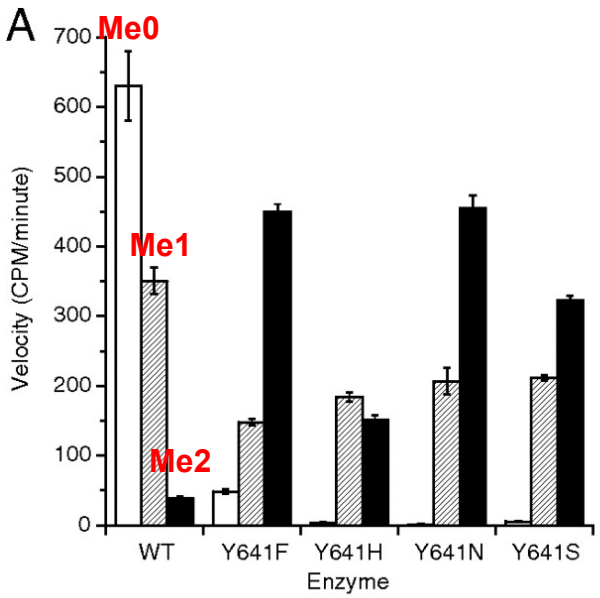

• Km Evaluation

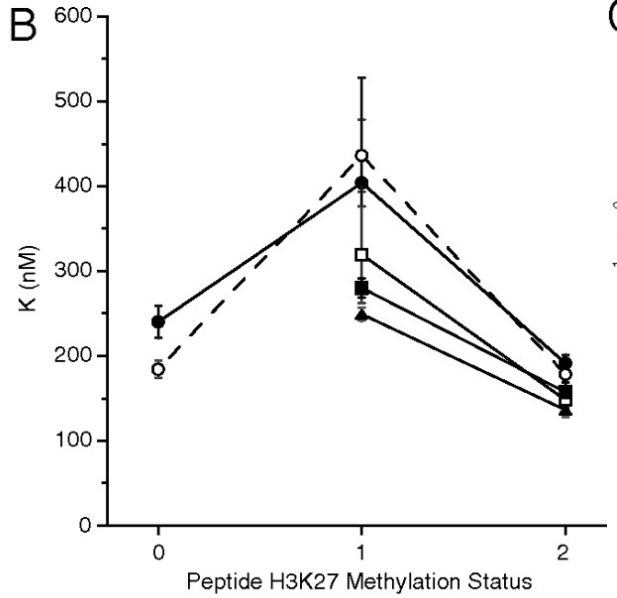

• Kcat Evaluation

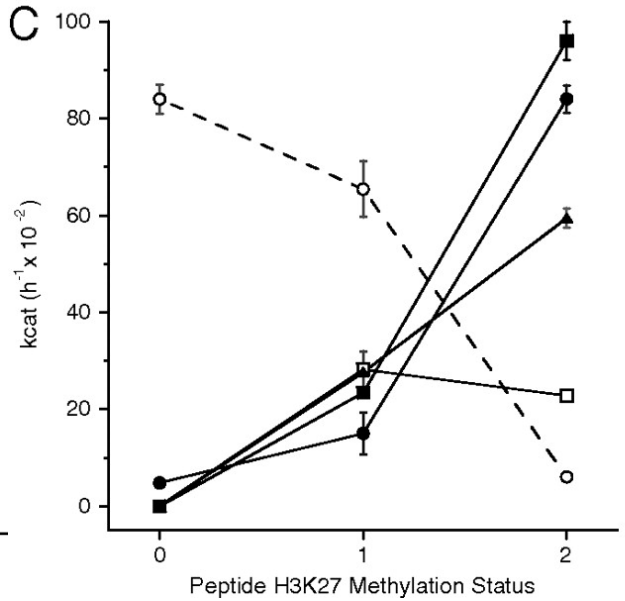

• Kcat/Km Evaluation

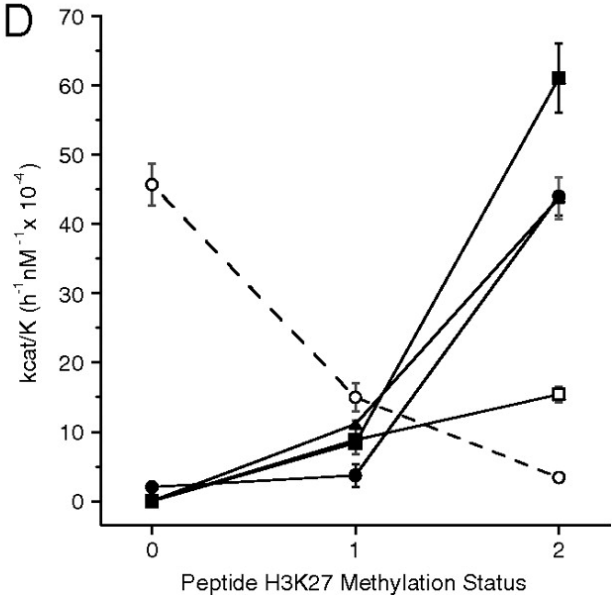

Wild-type (○),Y641F (•), Y641H (□), Y641N (▪), Y641S (▲)

WT EZH2 prefers H3K27Me0→1 reaction

Mutant EZH2 prefers H3K27Me1→2 or Me2→3 reaction

C. J. Sneeringer et al,Proc. *Natl. Acad. Sci*. **2010**,*107*,20980–510.

PRC2 complexes containing mutant EZH2 preferentially catalyze di- and trimethylation of histone H3K27. (A) Methyltransferase activity of mutant and WT complexes on unmethylated peptide (open bars), monomethylated peptide (hatched bars), and dimethylated peptide (closed bars). (B) Affinity for peptide substrates as defined by $K_{1/2}$ is similar across all peptide methylation states for PRC2 complexes containing wild-type (○),Y641F (•), Y641H (□), Y641N (▪), and Y641S (▲) EZH2. Note that the $K_{1/2}$ values across all substrates and all enzyme forms varies less than 3.5-fold. For any particular methylation state of substrate, the variation in $K_{1/2}$ value is less than 2-fold. (C) Enzyme turnover number (k_{cat}) varies with substrate methylation status in opposing ways for WT and Y641 mutants of EZH2. The k_{cat} decreases with increasing K27 methylation states for wild-type (○), but increases for Y641F (•), Y641H (□), Y641N (▪), and Y641S (▲) mutants of EZH2. (D) Catalytic efficiency ($k_{cat}/K_{1/2}$) decreases with increasing K27 methylation states for wild-type (○) but increases for Y641F (•), Y641H (□), Y641N (▪), and Y641S (▲) mutants of EZH2. (B–D) The lines drawn to connect the data points are not intended to imply any mathematical relationship; rather, they are intended merely to serve as a visual aid to guide the eye of the reader.

Appendix

- **Steps to generate EPZ005687**

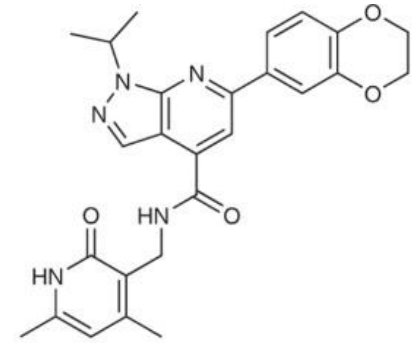

(**1**)
PRC2 K_i = 310 nM

Improve solubility

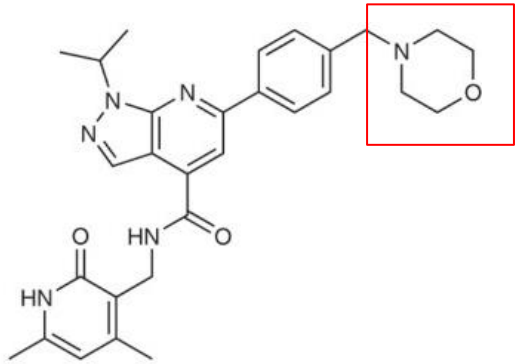

(**2**)
PRC2 K_i = 180 nM

Conversion to indazole

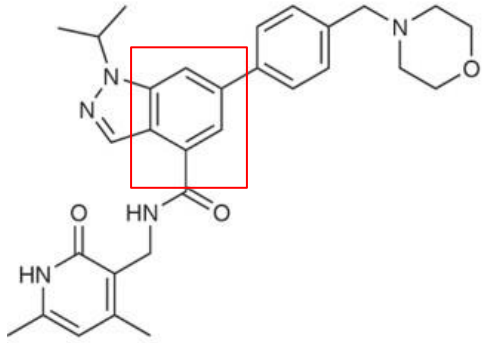

(**3**)
PRC2 K_i = 80 nM

Introduction of lipophilic group

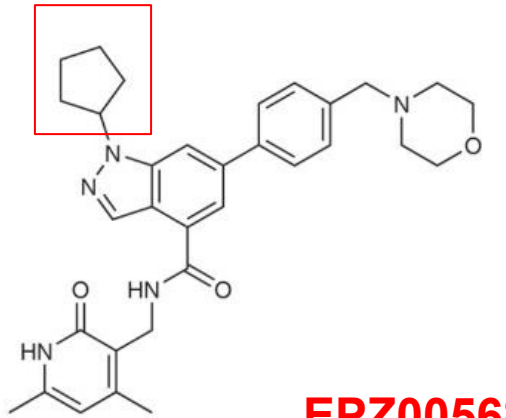

EPZ005687 (**4**)
PRC2 K_i = 24 nM

EPZ005687

Knutson, S et al, *Nat Chem Biol*, **2012**, *8*, 890.

Appendix

- Selectivity for H3K27

  - WT cell

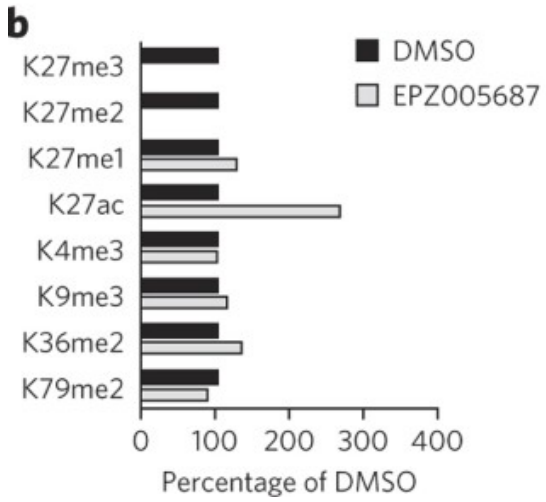

  - Y671F Mut cell

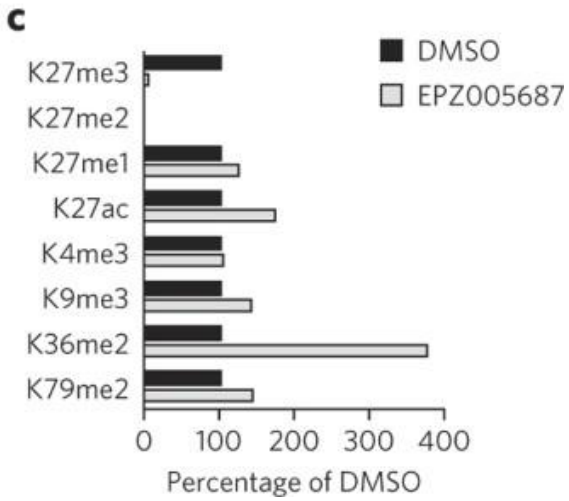

Appendix

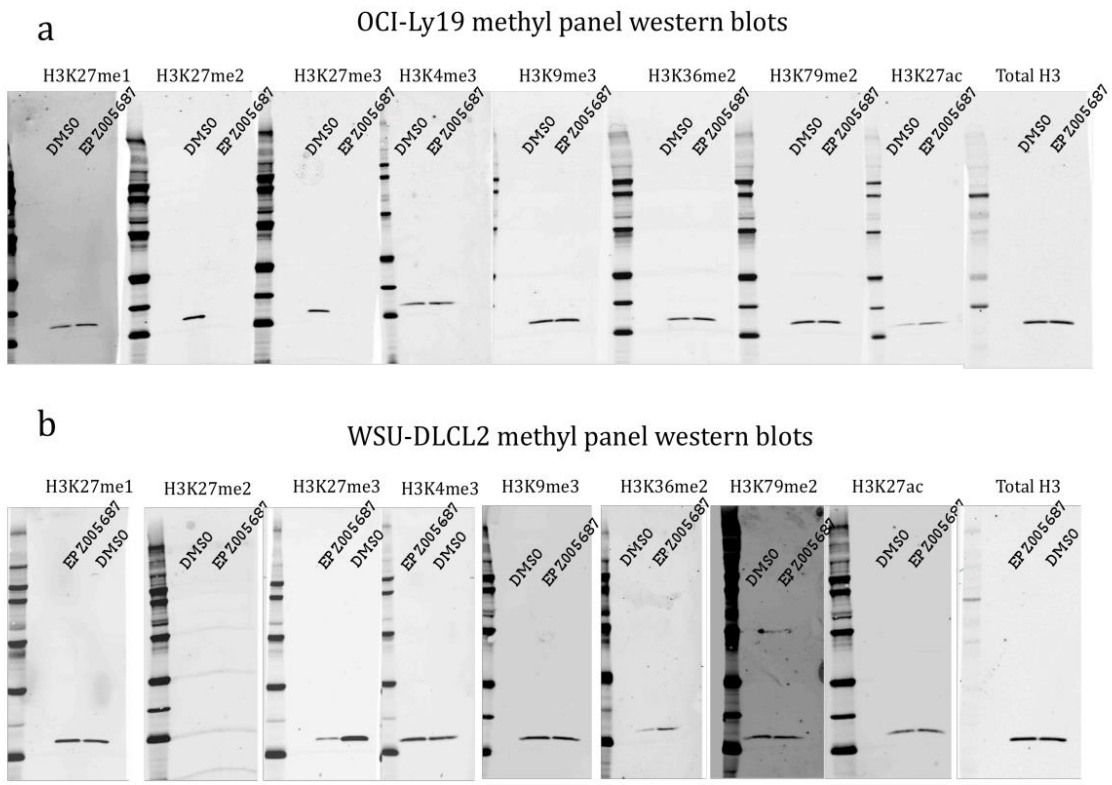

Supplementary Figure 4. Full western blots used for quantitation of methyl mark change in the OCI-Ly19 and WSU-DLCL2 cells treated with DMSO or EPZ005687. Quantitation of the OCI-Ly19 (a) and WSU-DLCL2 (b) blots was performed in the LiCor Odyssey software and the graphs are depicted in Figure 4b and 4c of the main text. Please note that each blot lane is labeled with DMSO or EPZ005687.

Appendix

- Effect on cell proliferation (G1) (tazemetostat)

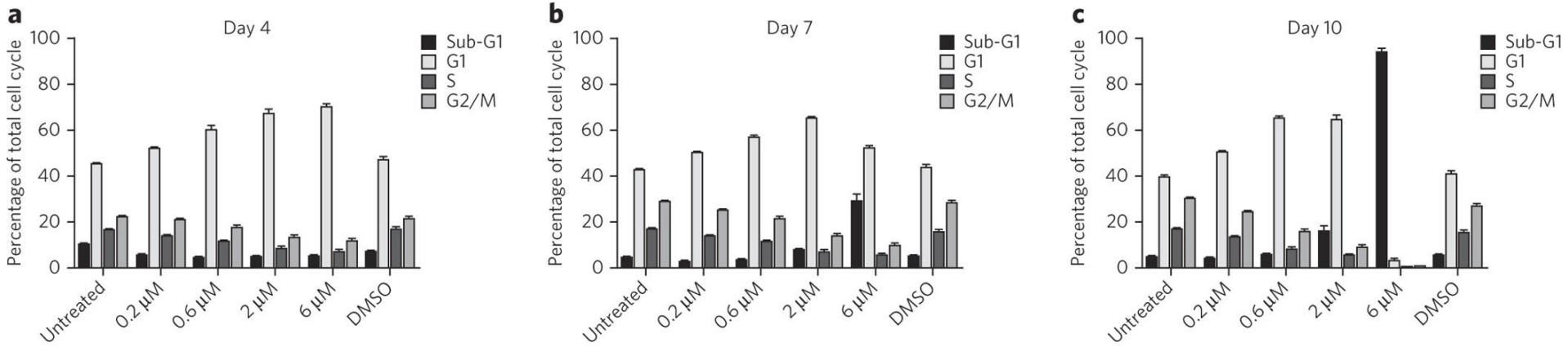

Appendix

Table 1. SAR Exploration of the R_1 Moiety[a,21]

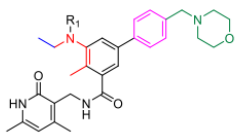

Compd.	R_1	EZH2 WT (IC_{50}: nM)	EZH2-Y641F (IC_{50}: nM)	WSU-DLCL2 (GI_{50}: μM)
1	/	11[21]	N/A	0.3 ± 0.1
2	/	12.9 ± 2.9	5.5 ± 1.7	5.0 ± 1.3

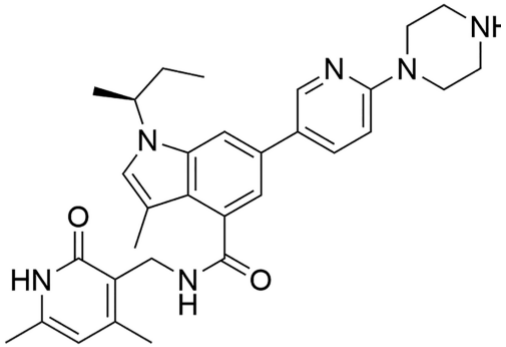

2 (GSK-126)

Table 2. SAR Exploration of the R_2 Moiety[a]

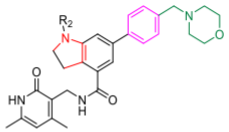

Compd.	R_2	EZH2 WT (IC_{50}: nM)	EZH2-Y641F (IC_{50}: nM)	WSU-DLCL2 (GI_{50}: μM)
15		396.4 ± 136.8	5290 ± 415	50.5 ± 8.8
16		394.2 ± 124.2	>10000	44.0 ± 14.1
17		238.1 ± 57.4	6240 ± 1530	51.6 ± 3.6
18		404.2 ± 69	6219 ± 3787	94.5 ± 19.1

[a]All IC_{50} values were obtained by triplet testing.

環　アミドでの検討

Bin Zhou et al, *J. Med. Chem.* **2021**, *64*, 15170.

Appendix

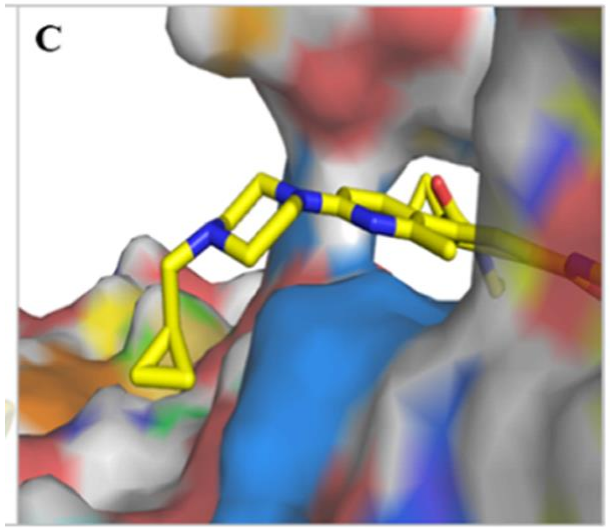

Table 3. SAR Exploration of the Tail Moiety[a]

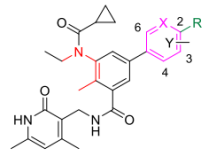

Compd.	X	Y	R	EZH2 WT (IC_{50}: nM)	EZH2-Y641F (IC_{50}: nM)	WSU-DLCL2 (GI_{50}: μM)
19	-	-	NH_2	19.1± 0.3	61.2 ± 1.7	0.8 ± 0.1
20	-	-		47.3 ± 5.3	150.3 ± 1.1	0.9 ± 0.3
21	-	-		40.7 ± 4.3	70.3 ± 2.7	0.8 ± 0.1
22	-	-		33.7 ± 1.3	49.6 ± 1.4	0.7 ± 0.4
23	-	-	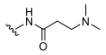	11.7 ± 0.1	34.9 ± 0	1.8 ± 0.4
24	-	-		37.6 ± 3.8	79.1 ± 3.3	0.2 ± 0.1
25	-	-		15.1 ± 0.9	33.1 ± 2.1	0.2 ± 0.1
26	-	-	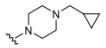	25.3 ± 0.6	50.5 ± 6.2	0.1 ± 0.1
27	-	-		16.0 ± 1.6	40.7 ± 3.3	0.2 ± 0.1
28	N	-	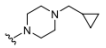	10.1 ± 0.7	24.4 ± 2.6	0.2 ± 0.1
29	N	6-Me	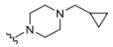	26.1 ± 1.3	72.3 ± 1.9	0.2 ± 0.1
30	N	3-Me	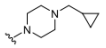	12.0 ± 1.5	30.4 ± 0.8	0.3 ± 0.1
31	N	4-Me	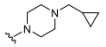	16.7 ± 1.2	40.4 ± 0.4	0.2 ± 0.1

[a]All IC_{50} values were obtained by triplet testing.

Bin Zhou et al, *J. Med. Chem.* **2021**, *64*, 15170.

Appendix

Table 4. Selected Analogues for Pharmacokinetic Profiling in Rats[a]

compd.	administration route	$T_{1/2}$ (h)	C_{max} (ng/mL)	$AUC_{0-\infty}$ (h*ng/mL)	V_z (mL/kg)	Cl (mL/(h kg))	F (%)
9	p.o. (10 mg/kg)	1.03 ± 0.29	473 ± 63	406 ± 207	53 401 ± 49 885	32 550 ± 23 359	15.1 ± 7.7
	i.v. (1 mg/kg)	0.38 ± 0.04	824 ± 88	269 ± 33	2034 ± 330	3760 ± 450	
11	p.o. (10 mg/kg)	1.88 ± 0.59	106 ± 136	244 ± 241	208 585 ± 156 684	69 942 ± 44 011	10.1 ± 10.0
	i.v. (1 mg/kg)	0.8 ± 0.1	686 ± 32	242 ± 16	4797 ± 696	4148 ± 270	
27	p.o. (10 mg/kg)	2.08 ± 1.04	115 ± 99	314 ± 272	470 567 ± 724 620	108 341 ± 146 360	13.0 ± 11.3
	i.v. (1 mg/kg)	1.55 ± 0.21	444 ± 49	241 ± 34	9318 ± 1072	4195 ± 549	
28	p.o. (10 mg/kg)	1.46 ± 0.11	67 ± 31	260 ± 73	84 455 ± 20 050	40 491 ± 11 092	9.4 ± 2.6
	i.v. (1 mg/kg)	1.25 ± 0.19	673 ± 128	277 ± 1	6499 ± 991	3616 ± 14	
29	p.o. (10 mg/kg)	1.45 ± 0.09	240 ± 102	604 ± 156	36 559 ± 10 975	17 441 ± 5221	31.0 ± 8.0
	i.v. (1 mg/kg)	1.23 ± 0.12	406 ± 27	195 ± 3	9104 ± 804	5130 ± 88	
30	p.o. (10 mg/kg)	1.82 ± 0.19	42 ± 18	132 ± 35	205 232 ± 44 436	9346 ± 350	4.8 ± 1.3
	i.v. (1 mg/kg)	1.79 ± 0.15	609 ± 78	277 ± 33	79 554 ± 23 108	3652 ± 455	

[a]Data are presented as the mean ± standard deviation (SD), n = 3; formulation: dimethyl sulfoxide (DMSO)/glucose solution (5% in water)/methyl sulfonic acid = 50:49.8:0.2.

Bin Zhou et al, *J. Med. Chem.* **2021**, *64*, 15170.

Appendix

Table 5. Inhibitory Effects of Compound 29 on HMT Activities[a]

HMTs	% activity	% inhibition (@10 μM)	HMTs	% activity	% inhibition (@10 μM)
G9a	100	0	SETDB1	99	1
GLP	104	0	SETD2	108	0
MLL1 complex	88	12	SET8	98	2
SET7/9	97	3	SMYD2	108	0
SUV39H1	99	1	SMYD3	84	16
SUV39H2	92	8	EZH1	8	92
PRMT1	93	7	EZH2	−1	100
PRMT3	104	0	EZH2 (A677G)	13	87
PRMT4	105	0	EZH2 (A738T)	−1	100
PRMT5	105	0	EZH2 (Y641S)	10	90
PRMT6	102	0	EZH2 (P132S)	−6	100
PRMT8	106	0	EZH2 (Y641C)	5	95
PRMT9	91	9	EZH2 (Y641F)	1	99
NSD1	88	12	EZH2 (Y641H)	19	81
NSD2	90	10	EZH2 (Y641N)	2	98
Dot1L	109	0	EZH2-EED	19	21
SUV4-20H1	100	0			

[a]Enzyme activity assays were performed in duplicates at each concentration. The luminescence data/α counts were analyzed and compared. In the absence of the compound, the intensity (C_e) in each data set was defined as 100% activity. In the absence of enzyme, the intensity (C_0) in each data set was defined as 0% activity. The percent activity in the presence of **29** was calculated according to the following equation: % activity = $(C - C_0)/(C_e - C_0)$, where C = the luminescence/α counts in the presence of **29**.

Bin Zhou et al, *J. Med. Chem.* **2021**, *64*, 15170.

Appendix

Table 9. In Vivo Pharmacokinetic Properties of 29 in Mice[a]

compd. **29**	$T_{1/2}$ (h)	C_{max} (ng/mL)	AUC_{0-t} (h*ng/mL)	$AUC_{0-\infty}$ (h*ng/mL)	V_z (mL/kg)	Cl (mL/(h kg))	F (%)
p.o. (10 mg/kg)	1.30	671	1002	1005	18 638	9954	27.0
i.v. (1 mg/kg)	5.38	1240	366	372	20 833	2685	

[a]Formulation: DMSO/glucose solution (5% in water)/methyl sulfonic acid = 50:49.8:0.2.

Bin Zhou et al, *J. Med. Chem.* **2021**, *64*, 15170.

Appendix

EZH1/2　両方阻害は有効？